Chapter 29

Continental-Scale Patterns in Neogene Mammal Community Evolution and Biogeography

A Europe-Asia Perspective

MAJID MIRZAIE ATAABADI, LI-PING LIU, JUSSI T. ERONEN, RAYMOND L. BERNOR, AND MIKAEL FORTELIUS

Spatial diachrony is a key question in stratigraphic correlation. If taxa appear at different times in different places, their first occurrences obviously will not represent useful time horizons. For terrestrial mammals, diachrony is closely intertwined with the question of faunal provinciality, including how provinces have themselves developed over time.

For Eurasia, the modern phase of research into diachrony and provinciality may be said to have begun with the 1975 Regional Committee on Mediterranean Neogene Stratigraphy meeting in Bratislava, Czechoslovakia. There, Pierre Mein produced his first iteration of his famous European Mammal Neogene (MN) zones (Mein 1975). This biochronologic system recognized reference faunas and struck correlations of European, North African, and West Asian vertebrate localities based on characteristic associations and first occurrences of taxa that migrated over great geographic distances in short intervals of geochronologic time. However, work in the Late Miocene of Maragheh, Iran (Bernor 1978, 1985, 1986), and Samos, Greece (Solounias 1981), developed biostratigraphic, biochronologic, and geochronologic work that did not support isochronic correlations of eastern Mediterranean/southwest Asian Turolian large mammal faunas with those of Europe (reviewed in Bernor, Solounias, et al. 1996 and Fortelius et al. 1996). This prompted Bernor and others (Bernor 1978; Bernor et al. 1979; Bernor 1984; Bernor and Pavlakis 1987) to propose several Eurasian and African biogeographic provinces that were distinct in their faunal character and ecology with resulting time-transgressive dispersion of successive chronofaunas (Olson 1952).

For a well-resolved answer to questions concerning temporal occurrence of fossil taxa, an independent chronology is necessary. That is to say, a chronology that is not based on the occurrence or evolution of the taxa concerned or on information that is likely to be correlated with those phenomena. In practice, this would mean a chronology that excludes biochronology, a constraint that still severely reduces the amount of data available for analysis. Here, we use a different approach. We accept all stratigraphic information of adequate quality as given in the NOW database (Fortelius 2009), including mammal biochronology, and investigate the spatial and temporal distribution of two attributes that reflect the regional development of faunas and environments: faunal resemblance and humidity estimated from mean hypsodonty. We ask whether within this biochronologically driven stratigraphic framework evidence still exists for diachronous development of faunas and environments in different regions. This is a conservative approach in that both faunal resemblance and hypsodonty depend on evolution over time, as does biochronology. If diachrony is nonetheless detected, the evidence for it must be regarded as strong.

Our two-pronged approach also allows us to ask whether the faunal resemblance patterns are related to

regional differences in environmental conditions. We have previously shown that the mean "ordinated hypsodonty" (i.e., molar crown height assigned to hypsodonty classes; see the following section on methods) of large herbivorous mammals indicates major regional differences in the general trend of Neogene midlatitude aridification (Fortelius et al. 2002, 2003, 2006), and that these patterns are due to the genera and species with the highest occupancy (relative locality coverage; Jernvall and Fortelius 2002). Very recently, we addressed the dynamics of land mammal provinciality using faunal similarity to chart the origin, rise, acme, decline and extinction of the Pikermian chronofauna between 12 Ma and 5 Ma. We showed that the westward expansion of the Pikermian chronofauna from the late Middle Miocene to the medial Late Miocene correlates closely with the expansion of arid habitats as well as with the output of a paleoclimate modeling study (Eronen et al. 2009). We used Olson's concept of chronofauna in a quantitative sense for a faunal assemblage defined by taxonomic similarity, as described in the "Data and Methods" section.

Here, we turn our attention to the development of the Middle and Late Miocene mammal assemblages of East Asia, which we refer to as the Tunggurian and Baodean chronofaunas, after their most classic localities of occurrence (Tunggur-Moergen and Baode). Well known as the "pre-*Hipparion*" and "*Hipparion* faunas" of China, they respectively became the bases of the Tunggurian and Baodean land mammal ages in East Asia (Li, Wu, and Qiu 1984; Qiu and Qiu 1990, 1995).

The recently reviewed faunal composition of Tunggur-Moergen and Baode locality 49 mammal localities is shown in table 29.1. The traditional Tunggur "*Platybelodon* fauna" has recently been appointed to the Tunggur-Moergen fauna, to distinguish it from the underlying Tairum Nor fauna (Qiu, Wang, and Li 2006). The Tunggur-Moergen locality, the paleomagnetic correlation for which is between chrons C5Ar.3r and C5r.3r (13–11.8 Ma; Wang, Qiu, and Opdyke 2003), is reported as being correlative with MN-equivalent 7+8 (Qiu, Wu, and Qiu 1999). The Baode Red Clay fauna as a whole is now correlated to MN-equivalent 13 (Zhang and Liu 2005; Kaakinen et al., chapter 7, this volume). The paleomagnetic age for the Baode Formation in the type area is 7.23–5.34 Ma (Zhu et al. 2008), with an estimated age for locality 49 at 7.0 Ma (Kaakinen et al., chapter 7, this volume). In this chapter, we have selected Tunggur-Moergen and Baode locality 49 as the type localities for the two chronofaunas.

DATA AND METHODS

We downloaded the dataset from the NOW database on April 24, 2009 (see http://www.helsinki.fi/science/now). We used all large mammal data between 20.5 Ma and 3.4 Ma, encompassing the European Neogene mammal units MN 3 to MN 15.

The final dataset as analyzed for similarity indices comprised 358 localities and 516 taxa and is available upon request from the authors. We calculated different Genus-level Faunal Resemblance Indices (GFRIs) to Baode locality 49 and Tunggur-Moergen locality from the dataset using PAST (Hammer, Harper, and Ryan 2001; Hammer and Harper 2006; see http://folk.uio.no/ohammer/past/). We used Dice, Jaccard, Simpson, and Raup-Crick GFRIs to compare differences in the overall trends and between different GFRIs. Dice FRI is highly recommended by Archer and Maples (1987) and Maples and Archer (1988) and is calculated as $2C/(A + B)$, where C is the number of shared taxa between two faunas, and A and B are the total number of taxa in the compared faunas. We mapped the results only for Dice GFRI and have presented other GFRI results (which show similar patterns) in the appendix.

We applied the following criteria for undertaking these analyses: localities were excluded when they (1) could not be assigned to the temporal span of a single "MN-equivalent" unit, (2) had fewer than 7 taxa identified at the genus level, or (3) lacked geographic positional data (coordinates). We tested our method with different minimum numbers of taxa. We found that when we used fewer than 7 taxa the analytical noise increased, and when we limited the analysis to localities with 10 or more taxa, the number of available localities was low. Overall, we found the number of taxa used did not affect the spatial geographic patterns.

As provisional common coinage for Eurasian mammal biostratigraphy, we use ad hoc "MN-equivalents" (MNEQ). These are defined and computed from minimum and maximum age estimates for the locality ages as given, according to where the computed range midpoint falls in the correlation scheme in use in the NOW database (Steininger et al. 1996). In this study, we only included localities where the age span is less than or equal to that of the corresponding MN unit.

Olson (1952, 1958) developed the concept of the chronofauna for "a geographically restricted, natural assemblage of interacting animal populations that has maintained its basic structure over a geologically

Table 29.1
Updated Faunal Lists of Tunggur-Moergen and Baode Locality 49

Order	Tunggur-Moergen[a]	Baode Locality 49[b]
Carnivora	*Amphicyon tairumensis*	*Amphicyon* indet.
	?*Melodon* indet.	?*Melodon incertum*
	Metailurus mongoliensis	*Melodon majori*
	Plithocyon teilhardi	*Metailurus parvulus*
	Pseudarctos indet.	*Felis* indet.
	Gobicyon macrognathus	*Machairodus palanderi*
	Mionictis indet.	*Megantereon* indet.
	Martes indet.	*Adcrocuta eximia*
	Tungurictis spocki	*Hyaenictitherium hyaenoides*
	Percrocuta tungurensis	*Hyaenictitherium wongii*
	Sansanosmilus indet.	*Ictitherium viverrinum*
		?*Lycyaena dubia*
		Lutra aonychoides
		Plesiogulo brachygnathus
		Promephitis cf. *maeotica*
		Proputorius minimus
Proboscidea	*Zygolophodon gobiensis*	*Mammut borsoni*
	Platybelodon grangeri	*Mammut* indet.
Perissodactyla	*Anchitherium gobiense*	*"Hipparion" plocodus*
	Chalicotherium brevirostris	*"Hipparion" platyodus*
	Acerorhinus zernowi	*"Hipparion" hippidiodus*
	Hispanotherium tungurense	*"Hipparion" coelophyes*
	Rhinocerotidae indet.	*"Hipparion"* indet.
		Acerorhinus palaeosinensis
		Chilotherium indet.
		Stephanorhinus orientalis
Artiodactyla	*Listriodon splendens*	?*Dorcadoryx lagrelii*
	Kubanochoerus indet.	*Gazella dorcadoides*
	Palaeotragus tungurensis	*Gazella gaudryi*
	Stephanocemas thomsoni	*Gazella* indet.
	Lagomeryx triacuminatus	*Gazella* ?*paotehensis*
	Euprox grangeri	*Palaeoryx sinensis*
	Dicrocerus indet.	*Urmiatherium intermedium*
	Micromeryx indet.	*Cervavitus novorossiae*
	Turcoceros grangeri	*Procapreolus latifrons*
	Turcoceros noverca	*Honanotherium schlosseri*
		Palaeotragus microdon
		Palaeotragus indet.
		Propotamochoerus hyotherioides
		Chleuastochoerus stehlini

[a]Wang, Qiu, and Opdyke (2003).

[b]Kaakinen et al. (chapter 7, this volume).

significant period of time" (Olson 1952:181). We define a computational equivalent of this concept in terms of faunal resemblance: a chronofauna is a set of localities united by faunal similarity to an arbitrarily selected type or standard locality. In this exploratory study, we have not set numerical limits to chronofaunas—although that would be possible—but have simply mapped and described the rise and fall of these entities over a series of time steps based on correlation with the MN system.

For hypsodonty calculations, we used only large herbivorous mammals; all small mammals (orders Lagomorpha, Chiroptera, Rodentia, and Insectivora) as well as carnivores (orders Carnivora and Creodonta) were deleted. Three classes of hypsodonty are recorded in the NOW database: brachydont, mesodont, and hypsodont. The criteria for assigning species to these classes are ultimately up to the taxonomic coordinators of the NOW advisory board, but the rule of thumb is based on the ratio of height to length of the second molar (upper or lower). Brachydont teeth have a ratio of less than 0.8, mesodont have a ratio in the range 0.8–1.2, and hypsodont over 1.2. For this study, the hypsodonty classes were assigned the values 1, 2, and 3, respectively. This is a relatively conservative procedure, as the difference in crown height between a hypsodont and a brachydont species is usually more than 3:1. The mean hypsodonty value (see appendix) was calculated for each locality by averaging these ordinated scores (excluding localities with a single species).

All maps depicting GFRI and hypsodonty values were made in MapInfo Professional 8.5 using the color grid interpolation and inverse distance weighted (IDW) algorithm with the following settings: cell size 20 km, search radius 600 km, grid border 600 km, number of inflections 10, values rounded to 0.01 (0.1 for hypsodonty) decimal. The inflection values were manually set to range from 1 to 3 for hypsodonty, from 0 to 0.55 for Baode FRI, and 0.5 for Tunggur FRI maps. We used opacity of 25% for the color interpolation to show the base map below the interpolated values.

"Hipparion" here is applied to all the species of hipparionine horses that are not explicitly assigned to any one of the following genera: *Hippotherium*, *Cremohipparion*, *Cormohipparion*, *Plesiohipparion*, or *Proboscidipparion*. We have presented the shared taxa between some major localities and also listed the genera with the highest incidence of occurrence in some time intervals in order to show the taxa driving the enhanced similarity patterns.

RESULTS

The Tunggurian chronofauna begins to emerge in MNEQ 4 (plate 29.1*B*), when the overall similarity to the Tunggur-Moergen locality is still low in all of Eurasia, as it was during the preceding interval, MNEQ 3 (see plate 29.1*A*). The Sihong-Songlinzhuang fauna (see plate 29.1*B* [SS]), shows a higher similarity to Tunggur (Dice 0.28) than European localities. It shares six genera with the Tunggur-Moergen fauna: *Anchitherium*, *Dicroceros*, *Lagomeryx*, *Micromeryx*, *Palaeotragus*, and *Stephanocemas*—all brachydont ungulates primarily associated with closed environments. Tunggur genera with the highest incidence of occurrence in the whole data matrix for MNEQ 4 are *Anchitherium*, *Amphicyon*, and *Lagomeryx*. Another region of emerging similarity is southwestern Europe (for geographical regions, see figure 29.1). Córcoles (see plate 29.1*B* [CC]), Spain (Dice 0.23) and Bézian (see plate 29.1*B* [BZ]), France (Dice 0.23) share *Amphicyon*, *Chalicotherium*, *Anchitherium*, *Hispanotherium*, *Lagomeryx*, *Martes*, *Mionictis*, *Plithocyon* and *Stephanocemas* with the Tunggur-Moergen fauna. The humidity analysis from hypsodonty (see plate 29.1*I*) suggests that East Asia (see figure 29.1) was humid at this time (blue pattern of East Asia in plate 29.1*I*), with incipient aridification in western Europe (notice the green pattern of southwestern Europe in plate 29.1*I*). This indicates that the "*Hispanotherium* fauna," which inhabited the seasonal dry conditions of the lower Middle Miocene of the Iberian peninsula in Europe (Antunes 1979; Agusti and Anton 2002), had not yet extended to East Asia.

More Tunggurian elements appear in MNEQ 5 (see plate 29.1*C*); the genera with the highest incidence of occurrence are *Anchitherium*, *Amphicyon*, and *Lagomeryx*. The highest similarity to Tunggur is found for Esvres-Marine Faluns (see plate 29.1*C* [EMF]), France (Dice 0.38), and the second highest for Kalkaman Lake (see plate 29.1*C* [KL]), Kazakhstan (Dice 0.33). There are 13 Tunggur-Moergen genera at Esvres-Marine Faluns, a significant component of western origin and some immigrant taxa, including *Hispanotherium*, *Chalicotherium*, *Anchitherium*, *Lagomeryx*, *Dicrocerus*, *Euprox*, *Amphicyon*, *Martes*, *Mionictis*, *Plithocyon*, *Pseudarctos*, *Sansanosmilus*, and *Zygolophodon*. In China, the Shanwang (see plate 29.1*C* [SW]) fauna (Dice 0.18) retains *Lagomeryx* and *Stephanocemas* from Sihong-Songlinzhuang fauna, suggesting that the climate and environment remained stable with little change in humidity (see plate 29.1*J*).

The maximum extent of the Tunggurian chronofauna occurred in MNEQ 6 (see plate 29.1*D*). Hezheng-Laogou

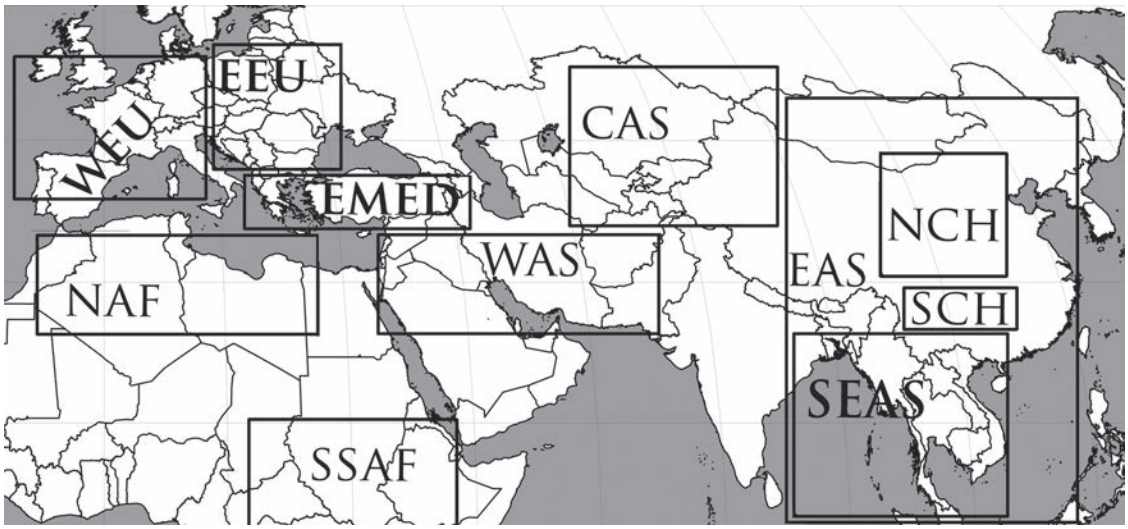

Figure 29.1 Geographical regions applied in this chapter. WEU = western Europe; EEU = eastern Europe; EMED = eastern Mediterranean; WAS = western Asia; CAS = central Asia; EAS = eastern Asia; SEAS = southeast Asia; NCH = North China; SCH = South China; NAF = North Africa; SSAF = Sub-Saharan Africa.

(see plate 29.1*D* [HL]) in China has the highest similarity to Tunggur (Dice 0.5), while high similarity is also seen for the locality Sansan (see plate 29.1*D* [S]), France (Dice 0.35), as well as Catakbagyaka (see plate 29.1*D* [CB]), Turkey (Dice 0.32), and Tongxin-Dingjiaergou (see plate 29.1*D* [TD]), China (Dice 0.32). The genera with the highest incidence of occurrence are *Anchitherium*, *Listriodon*, and *Amphicyon*. According to the hypsodonty proxy, humidity is uniform in Eurasia at this time with the exception of Ayibaligi Mevkii locality (see plate 29.1*K* [AM]) in Turkey, which shows dry conditions (red pattern).

During MNEQ 7+8, the low number of localities with high similarity to Tunggur indicates that the Tunggurian elements decline, except of course in Tunggur-Moergen itself (see plate 29.1*E* [TM]). The genera with the highest incidence of occurrence are *Listriodon*, followed by *Euprox*, *Micromeryx*, and *Chalicotherium*. At this time, the latitudinal climate gradient increased and arid belts appeared in the mid-latitudes of Asia (Flower and Kennett 1994; Liu, Eronen, and Fortelius 2009). In addition, eastern Mediterranean and eastern Europe (see figure 29.1) became more arid (notice the yellow patterns in plate 29.1*L*). The sparse data from southern East Asia (Chiang Muan [see plate 29.1*E* (CM)], Thailand) show significant difference from Tunggur-Moergen (Dice 0, no shared taxa). Although both areas have yielded primate-bearing faunas, the northern Tunggur and southern Chiang Muan faunas are now separated by an arid belt (yellow pattern of East Asia in plate 29.1*L*) and have fully dissimilar faunas.

In MNEQ 9, the Tunggurian signal has essentially vanished from Eurasia (mostly blue patterns of no significant similarity in plate 29.1*F*), with some lingering similarity still seen in western Europe, including Spanish localities like Can Ponsic I (see plate 29.1*F* [CP]) (Dice 0.29) and Can Llobateres I (see plate 29.1*F* [CL]; Dice 0.23). The mid-latitude drying in Asia and the eastern Mediterranean area continued in MNEQ 9 (orange/red patterns in plate 29.1*M*) and coincided with a replacement of the Tunggurian chronofauna by a "*Hipparion* fauna" of Late Miocene aspect. In MNEQ 10, even the low similarity in western Europe disappears (dominance of blue patterns in plate 29.1*G*). The continued drying and cooling in this area (yellowish patterns in plate 29.1*N*) causes the extinction of the remaining Middle Miocene taxa in western Europe known as the Vallesian Crisis (Agustí and Moya-Sola 1990; Agustí and Anton 2002; Agustí, Sanz de Siria, and Garcés 2003) at the MN 9–10 boundary. In East Asia, continued drying of MNEQ 10 favored the expansion of the "*Hipparion* fauna" (plate 29.2*B*).

The Baodean chronofauna is the East Asian expression of the Pan-Eurasian "*Hipparion* fauna" (Kurtén 1952),

corresponding to its western counterpart the Pikermian chronofauna (Eronen et al. 2009). At the beginning of the Late Miocene (MNEQ 9), genus similarity to Baode locality 49 (see plate 29.2*E* [B]) was still low across Eurasia (blue pattern dominant in plate 29.2*A*). *Adcrocuta*, *Gazella*, "*Hipparion*," *Ictitherium*, and *Machairodus* appear in China, while *Chilotherium*, *Gazella*, "*Hipparion*," and *Palaeotragus* appear at Sinap in Central Anatolia (see plate 29.2*A* [S]). The increasing aridification of the continent (orange/red patterns in plate 29.2*H*) favored expansion of open habitats and open-adapted taxa. *Gazella*, "*Hipparion*," and *Ictitherium* had reached the western margin of Eurasia at this time (Subsol de Sabadell [see plate 29.2*A* (SS)], Spain).

In MNEQ 10, more Baodean elements (e.g., "*Hipparion*," *Chilotherium*, *Gazella*, *Palaeotragus*, *Acerorhinus*, *Adcrocuta*, *Ictitherium*, *Machairodus*, *Hyaenictitherium*, and *Indarctos*) appear in Asia and in the eastern Mediterranean–West Asian region. Both North Chinese localities at this time show high similarity to Baode locality 49 (notice the orange pattern of northern China in plate 29.2*B*, which indicates Dice > 0.3), as do Grebeniki (see plate 29.2*B* [G]), Ukraine, and Poksheshty (see plate 29.2*B* [P]), Moldova (Dice > 0.35). The Baodean genera like *Adcrocuta*, *Cervavitus*, *Chilotherium*, *Gazella*, *Honanotherium*, "*Hipparion*," *Ictitherium*, *Machairodus*, *Metailurus*, *Palaeotragus*, *Plesiogulo*, and *Promephitis* appear widely in Eurasia, except for western Europe. The low similarity in western Europe may be related to its more humid climate (notice the blue/green pattern of western Europe in plate 29.2*I*) and the later expansion of the Pikermian chronofauna there (Eronen et al. 2009). The genera with the highest incidence of occurrence at this time across Eurasia are *Gazella*, "*Hipparion*," *Chilotherium*, and *Palaeotragus*.

The pattern in MNEQ 11 is similar to MNEQ 10 for the faunal similarity (see plate 29.2*C*), but for humidity, expansion of arid areas is observed (increase in yellow/orange patterns in plate 29.2*J*). The genera with the highest incidence of occurrence at this time are *Gazella*, "*Hipparion*," *Chilotherium*, *Palaeotragus*, and *Adcrocuta*. In addition to northern Chinese localities, Karacahasan (K), Kemiklitepe 1, 2 (KT), and Garkin (G) in Turkey, Thermopigi (T) in Greece, and Novaja Emetovka (NE) in Ukraine also show a high similarity (Dice > 0.3) to Baode locality 49 (see plate 29.2*C*). Western Europe still retains a remarkably low similarity to Baode locality 49 at this time (notice blue patterns of western Europe in plate 29.2*C*), and in addition, South China is dissimilar to North China (see figure 29.1 and plate 29.2*C*: notice light blue pattern in southern China compared to orange/red pattern in North China).

During the middle Turolian (MNEQ 12), the genera with the highest incidence of occurrence are *Gazella*, "*Hipparion*," *Palaeotragus*, and *Adcrocuta*. The Baodean signal in the Europe–West Asian region grows stronger, with more localities showing higher similarity to Baode locality 49 (green/yellow pattern in plate 29.2*D*). This is the time when the Pikermian chronofauna had its maximum geographic range in Eurasia (Eronen et al. 2009). Surprisingly, the similarity in China itself appears significantly reduced, with lower similarities (green pattern in plate 29.2*D*) than the previous time slice, although sampling is admittedly sparse. In North China, *Dorcadoryx*, *Lantiantragus*, *Shaanxispira*, *Schansitherium*, and *Dinocrocuta* appear (Lantian locality 6; see plate 29.2*D* [L]). *Dinocrocuta* is apparently a western element, but the large bovids and giraffes are all endemic genera. Such significant endemism in North China was previously found for species and genera of rodents and ungulates by Fortelius and Zhang (2006). In South China, some western elements do appear, and the similarity accordingly rises somewhat (green pattern in plate 29.2*D*). From MNEQ 11 to MNEQ 12, North China is among the driest areas in Eurasia (notice red patterns in plate 29.2*J–K*), and the endemic Chinese ruminant fauna seems to have evolved in response to these regionally harsh conditions (Fortelius and Zhang 2006).

During MNEQ 13, the genera with the highest incidence of occurrence are still "*Hipparion*," *Gazella*, and *Adcrocuta*. With the onset of red clay deposition at about 7 Ma (Sun et al. 1998; Qiang et al. 2001; Zhu et al. 2008; Kaakinen et al., chapter 7, this volume), approximately correlative with the beginning of MNEQ 13, the mammal record of North China improves dramatically (more North Chinese localities in plate 29.2*E*). The immigration of genera from adjoining areas results in a large area of high similarity across north central Asia and North China (notice red patterns of these areas in plate 29.2*E*). The change coincides with a marked increase in humidity (green patterns of plate 29.2*L*) in northern China, interpreted as a result of a strengthening Asian Monsoon by Fortelius et al. (2002). In contrast to northern China, northern central Asia is dry at this time (orange pattern of this region in plate 29.2*L*). Similarity in the western part of the continent, where conditions in contrast appear drier in this interval, is now reduced (compare orange patterns of western Europe in plate 29.2*L* with green patterns of same region in plate 29.2*E*).

As far as the poor record suggests, the Baodean chronofauna declines drastically and is effectively gone during MNEQ 14–15 (no reddish pattern present in North China and northern central Asia in plate 29.2*F–G*). This

is despite little change in humidity of central Asia and China in MNEQ 14 (see yellow/red patterns of these regions in plate 29.2*M*).

DISCUSSION

It appears that the regionally differentiated history of environmental change is matched by patterns of diachronity in faunal similarity, even within a mainly biochronologic framework expected to minimize diachrony in species ranges. As a general finding, this is neither unexpected nor does it have new methodological implications for biostratigraphy. The details are more interesting and also potentially of greater practical concern.

The two cases that we have described here are quite different. The Tunggurian chronofauna appears to have originated in and extended from western Europe (yellow/orange/red patterns in plate 29.1*B–E*), where its early incarnation in the late Early/lower Middle Miocene is often referred to as the "*Hispanotherium* fauna." Its strongest expression in East Asia (orange/red patterns of this region in plate 29.1*D–E*) was at the very end of its history, in the terminal Middle Miocene, when it had already disappeared from other parts of its earlier range (see low similarity patterns of western Europe in plate 29.1*D–E*). In broad terms, this chronofauna seems to have first developed as a response to continental drying and increased seasonality (seasonal dryness) in Western Europe (notice green/orange patterns of this region in plate 29.1*I–J*), and to have followed the widening arid belt toward the east (red/yellow patterns in plate 29.1*K–L*). Its successive retreat from the western part of its range seems to reflect increased humidity in western Europe (notice blue patterns in plate 29.1*K–L*), which would have favored forest adapted taxa. It may also have been impacted by the increased aridity in the eastern Mediterranean (see red/yellow pattern of this region in plate 29.1*K–L*), which evidently drove the concurrent emergence of the Pikermian chronofauna there. Similarly, its ultimate extinction in East Asia (note the demise of yellow/red patterns in plate 29.1*F–G* and emergence of orange patterns in plate 29.2*B*) also seems to coincide with the expansion of the Pikermian-like Baodean chronofauna.

The protracted extension of the Tunggurian chronofauna across Eurasia (see change in location of yellow/orange patterns in plate 29.1*C–D*) implies a continuum of similar environments across its geographic range. Such a continuum is suggested by the remarkable uniformity of the Eurasian mammal fauna in MNEQ 6 (plate 29.1*D*, notice the yellow/red pattern). Whether this reflects the lingering biogeographic effects of the immediately preceding Mid-Miocene Climatic Optimum (climax time of Neogene warmth between 17 Ma and 15 Ma) or whether it is a direct result of the contemporary Mid-Miocene Cooling event between 14.8 Ma and 14.1 Ma (Flower and Kennett 1994; Zachos et al. 2001; Böhme 2003) is currently difficult to assess. In MNEQ 7+8, the overall similarity definitely declines with low number of localities with high similarity to the Tunggur locality (fewer yellow/red patterns in plate 29.1*E*) compared to the next older time slice (see plate 29.1*D*). This is coincidental with the incipient development of mid-latitude aridity (yellow patterns in plate 29.1*L*) as the cooling trend continues. In this perspective, the Tunggur-Moergen fauna (see plate 29.1*E* [TM]) appears as a last remnant of the Tunggurian chronofauna in a stable environment, which in the context of overall mid-latitude drying (Liu, Eronen, and Fortelius 2009) appears relatively humid (notice the light-blue pattern of Tunggur locality [TM] in plate 29.1*L*).

The history of the Baodean chronofauna is quite different. Although part of the Pan-Eurasian "*Hipparion* fauna" (Kurtén 1952), the Baodean chronofauna is distinct from the Pikermian chronofauna in its taxonomic content. The mature Northeast Asian Baodean chronofauna has a high proportion of immigrants compared with its precursors (Fortelius and Zhang 2006) and differs from the West Eurasian Pikermian chronofauna by relative diversity and abundance of mustelids, rhinocerotids, and cervids in combination with rarity of primates, giraffids, and mastodonts (Deng 2006). In part this may simply reflect its younger age, but growing evidence is emerging that the difference is also an expression of the relatively high endemism of this chronofauna, strongly dominated by ruminant and equid lineages that extend from the eastern Mediterranean and Balkans to China (Fortelius and Zhang 2006; Watabe 1992). In fact, vicariant East Asian radiations paralleling the West Asian (Pikermian) ones may be more common than has been recognized previously—for example, among the hipparionine horses (Bernor, Koufos, et al. 1996) and aceratherine rhinoceroses (Fortelius et al. 2003). Hipparionine horses in particular show long-distance extensions across this range and include species belonging to the genera *Hipparion*, *Cremohipparion* and later, *Plesiohipparion*. In the Late Miocene, geographic extension of *Hipparion* (especially *Hipparion dietrichi* and *Hipparion campbelli*) and *Cremohipparion* (*Cr. moldavicum*, *Cr. mediterraneum*, *Cr. proboscideum*, and *Cr. matthewi*) from western Eurasia to East Asia (*Hipparion hippidiodus* and *Cr. licenti*) would appear to have been followed by vicariance.

In contrast to the Tunggurian chronofauna, the Baodean chronofauna thus seems to have developed via a stage-of-endemism in a harsh environmental setting, followed by expansion when summer rainfall brought richer resources and immigrants to northern China in the latest Miocene. It peaked in its species diversity significantly later (MNEQ 13) than the Pikermian chronofauna (MNEQ 12), but on current evidence neither Pikermian (Eronen et al. 2009) nor Baodean chronofaunas continued into the Pliocene (vanished yellow/red pattern in plate 29.2*F*–*G*). The slower fall of the Baodean chronofauna in North China possibly benefited from little change in the humid conditions before 4 Ma as suggested by red clay lithology (Ding et al. 1999; Vandenberghe et al. 2004), fossil molluscs (Wu et al. 2006), pollen records (Wang et al. 2006), dust flux in the North Pacific (Rea, Snoeckx, and Joseph 1998), and isotopic evidence (Passey et al. 2008). An interesting contrast is the Yushe Basin (see plate 29.2*F* [Y]) hipparions, which included advanced members of the Late Miocene Pikermian and Baodean lineages (*Cremohipparion licenti*) as well as endemic Chinese lineages (*Proboscidipparion pater* and *Plesiohipparion houfenense*; Qiu, Huang, and Guo 1987).

Buildup of the similarity of mammal species across the known range of Pikermian chronofaunas, from China in the east, to Europe in the west, and to northern and Sub-Saharan Africa in the southwest (Bernor, Rook, and Haile-Selassie 2009) likely happened as a result of a large number of more or less independent range extensions, with diachronity in both appearances and extinctions of discrete mammalian lineages. The end-Miocene decline and base-Pliocene extinction of Pikermian chronofaunas was evidently a much more definite event, with ultimate extinction virtually instantaneous in a biochronological sense (Eronen et al. 2009). Chronofaunas, like individual species and genera, typically appear to have unimodal histories including buildup, climax, and decline. However, in contrast to the individual genera and species of these faunas, where rise and fall appear symmetrical (Jernvall and Fortelius 2004), the decline of the two chronofaunas investigated here appears significantly more abrupt than their gradual buildup.

Both the Tunggurian and the Baodean chronofaunas moved into East Asia from the west. Although the details are different, these chronofaunas apparently moved across the continent in response to changing climate (humidity). This appears to be the case of expansion as well as contraction. Despite the underlying assumption of taxonomic isochrony, the standard biochronologic framework does appear to be stable enough to reveal regionally diachronous change at the continental scale. This is strong evidence that taxon ranges are generally highly diachronous across Eurasia.

ACKNOWLEDGMENTS

We thank the Academy of Finland for project funding on long-term work in China (to MF). LPL is indebted to the support from the Major Basic Research Projects of MST of China (2006CB806400), the NSFC (40872018, 40672010), and State Key Laboratory of Paleobiology and Stratigraphy (Nanjing Institute of Geology and Paleontology, CAS, No.083114). JTE and LPL acknowledge funding support from Kone Foundation. RLB wishes to acknowledge funding from the National Science Foundation, including EAR0125009 and BCS-0321893 (Revealing Hominid Origins Initiative to F. Clark Howell and Tim White). We thank Anu Kaakinen, Zhaoqun Zhang, and Ben Passey for discussions. We are also grateful to Michael Woodburne and Nikos Solounias for their productive reviews and helpful comments.

REFERENCES

Agustí, J. and M. Antón. 2002. *Mammoths, Sabertooths, and Hominids*. New York: Columbia University Press.

Agustí, J. and S. Moya-Sola. 1990. Mammal extinctions in the Vallesian (Upper Miocene). *Lecture Notes in Earth Science* 30:425– 432.

Agustí, J., A. Sanz de Siria, and M. Garcés. 2003. Explaining the end of the hominoid experiment in Europe. *Journal of Human Evolution* 45(2):145–153.

Antunes, M. T. 1979. *Hispanotherium* fauna in Iberian Middle Miocene, its importance and paleogeographical meaning. *Annales Geologiques Des Pays Helleniques*, non-series vol. 1:19–26.

Archer, A. W. and C. G. Maples. 1987. Monte Carlo simulation of selected binomial similarity coefficients (1): Effect of number of variables. *Palaios* 2:609–617.

Bernor, R. L. 1978. The mammalian systematics, biostratigraphy and biochronology of Maragheh and its importance for understanding Late Miocene hominoid zoogeography and evolution. Ph.D. diss., University of California, Los Angeles.

Bernor, R. L. 1984. A zoogeographic theater and a biochronologic play: The time/biofacies phenomena of Eurasian and African Miocene mammal provinces. *Paléobiologie Continentale* 14:121–142.

Bernor, R. L. 1985. Systematic and evolutionary relationships on the hipparionine horses from Maragheh, Iran (Late Miocene, Turolian age). *Palaeovertebrata* 15:173–269.

Bernor, R. L. 1986. Mammalian biostratigraphy, geochronology, and zoogeographic relationships of the Late Miocene Maragheh fauna, Iran. *Journal of Vertebrate Paleontology* 6:76–95.

Bernor, R. L., P. A. Andrews, N. Solounias, and J. A. van Couvering. 1979. The evolution of "Pontian" mammal faunas: Some zoogeographic, palaeoecological and chronostratigraphic considerations. *Annales Pays Helleneniques*, non-ser. vol. 1:81–89.

Bernor, R. L., G. D. Koufos, M. O. Woodburne, and M. Fortelius. 1996. The evolutionary history and biochronology of European and South West Asian Late Miocene and Pliocene Hipparionine horses. In *The Evolution of Western Eurasian Neogene Mammal Faunas*, ed. R. L. Bernor, V. Fahlbusch, and H. W. Mittmann, pp. 307–338. New York: Columbia University Press.

Bernor, R. L. and P. P. Pavlakis. 1987. Zoogeographic relationships of the Sahabi large mammal fauna. In *Neogene Paleontology and Geology of Sahabi*, ed. N. T. Boaz, A. El-Arnauti, A. W. Gaziry, J. De Heinzelin and D. D. Boaz, pp. 349–384. New York: Liss.

Bernor, R. L., L. Rook, and Y. Haile-Selassie. 2009. Paleobiogeography. In *Ardipithecus kadabba: Late Miocene Evidence from the Middle Awash, Ethiopia*, ed. Y. Haile-Selassie and G. Wolde Gabriel, pp. 549–563. Berkeley: University of California Press.

Bernor, R. L., N. Solounias, C. C. Swisher III, and J. A. Van Couvering. 1996. The correlation of three classical "Pikermian" mammal faunas—Maragheh, Samos and Pikermi—with the European MN unit system. In *The Evolution of Western Eurasian Neogene Mammal Faunas*, ed. R. L. Bernor, V. Fahlbusch, and H. W. Mittmann, pp. 137–156. New York: Columbia University Press.

Böhme, M. 2003. Miocene climatic optimum: Evidence from lower vertebrates of Central Europe. *Palaeogeography, Palaeoclimatology, Palaeoecology* 195: 389–401.

Deng, T. 2006. Paleoecological comparison between Late Miocene localities of China and Greece based on *Hipparion* faunas. *Geodiversitas* 28(3):499–516.

Ding, Z. L., S.-f. Xiong, J.-m. Sun, S.-l. Yang, Z.-y. Gu, and T.-s. Liu. 1999. Pedostratigraphy and paleomagnetism of a ~7.0 Ma eolian loess–red clay sequence at Lingtai, Loess Plateau, North-Central China and the implications for paleomonsoon evolution. *Palaeogeography, Palaeoclimatology, Palaeoecology* 152:49–66.

Eronen, J. T., M. Mirzaie Ataabadi, A. Micheels, A. Karme, R. L. Bernor, and M. Fortelius. 2009. Distribution history and climatic controls of the Late Miocene Pikermian chronofauna. *Proceedings of the National Academy of Sciences* 106(20):11867–11871.

Flower, B. P. and J. P. Kennett. 1994. The Middle Miocene climatic transition: East Antarctic ice sheet development, deep ocean circulation and global carbon cycling. *Palaeogeography, Palaeoclimatology, Palaeoecology* 108:537–555

Fortelius, M. (coordinator). 2009. *Neogene of the Old World Database of Fossil Mammals (NOW).* University of Helsinki. http://www.helsinki.fi/science/now/.

Fortelius, M., J. T. Eronen, L. Liu, D. Pushkina, J. Rinne, A. Tesakov, I. Vislobokova, Z. Zhang, and L. Zhou. 2002. Fossil mammals resolve regional patterns of Eurasian climate change during 20 million years. *Evolutionary Ecology Research* 4:1005–1016.

Fortelius, M., J. T. Eronen, L. Liu, D. Pushkina, A. Tesakov, I. Vislobokova, and Z. Zhang. 2003. Continental-scale hypsodonty patterns, climatic palaeobiogeography, and dispersal of Eurasian Neogene large mammal herbivores. In *Distribution and Migration of Tertiary Mammals in Eurasia, a Volume in Honour of Hans de Bruijn*, ed. J. Reumer and W. Wessels, pp. 1–11. DEINSEA 10.

Fortelius, M., J. T. Eronen, L. Liu, D. Pushkina, A. Tesakov, I. Vislobokova, and Z. Zhang. 2006. Late Miocene and Pliocene large land mammals and climatic changes in Eurasia. *Palaeogeography, Palaeoclimatology, Palaeoecology* 238: 219–227.

Fortelius, M., L. Werdelin, P. Andrews, R. L. Bernor, A. Gentry, L. Humphrey, H. W. Mittmann, and S. Viranta. 1996. Provinciality, diversity, turnover, and paleoecology in land mammal faunas of the later Miocene of Western Eurasia. In *The Evolution of Western Eurasian Neogene Mammal Faunas*, ed. R. L. Bernor, V. Fahlbusch, and H. W. Mittmann, pp. 414–448. New York: Columbia University Press.

Fortelius, M. and Z. Zhang. 2006. An oasis in the desert? History of endemism and climate in the Late Neogene of North China. *Palaeontographica A* 277:131–141.

Hammer, Ø. and D. A. T. Harper. 2006. *Paleontological Data Analysis.* Oxford: Blackwell.

Hammer, Ø., D. A. T. Harper, and P. D. Ryan. 2001. PAST: Paleontological Statistics Software Package for Education and Data Analysis. *Palaeontologia Electronica* 4(1): 9 pp.; http://palaeo-electronica.org/2001_1/past/past.pdf.

Jernvall, J. and M. Fortelius. 2002. Common mammals drive the evolutionary increase of hypsodonty in the Neogene. *Nature* 417:538–540.

Jernvall, J. and M. Fortelius. 2004. Maintenance of trophic structure in fossil mammal communities: Site occupancy and taxon resilience. *American Naturalist* 164:614–624.

Kurtén, B. 1952. The Chinese *Hipparion* fauna. *Commentationes Biologicae Societatis Scientiarum Fennicae* 13:1–82.

Li, C.-k., W.-y. Wu, and Z.-d. Qiu. 1984. Chinese Neogene: Subdivision and correlation. *Vertebrata PalAsiatica* 22(3):163–178.

Liu, L., J. T. Eronen, and M. Fortelius. 2009. Significant mid-latitude aridity in the Middle Miocene of East Asia. *Palaeogeography, Palaeoclimatology, Palaeoecology* 279:201–206.

Maples, C. G. and A. W. Archer. 1988. Monte Carlo simulation of selected binomial similarity coefficients (II): Effect of number of sparse data. *Palaios* 3:95–103.

Mein, P. 1975. In *Report on Activity of the RCMNS Working Group (1971–1975)*, ed. J. Senes, pp. 78–81. Bratislava, Slovakia: I.U.G.S. Commission on Stratigraphy, Subcommission on Neogene Stratigraphy.

Olson, E. C. 1952. The evolution of Permian Vertebrate Chronofauna. *Evolution* 6:181–196.

Olson, E. C. 1958. Fauna of the Vale and Choza: A summary, review and integration of the geology and faunas. Fieldiana. *Geology* 10 (32):397–448.

Passey, B. H., L. K. Ayliffe, A. Kaakinen, Z.-q. Zhang, J. T. Eronen, Y.-m. Zhu, L.-p. Zhou, T. E. Cerling, and M. Fortelius. 2008. Strengthened East Asian summer monsoons during a period of high-latitude warmth? Isotopic evidence from Mio-Pliocene fossil mammals and soil carbonates from northern China. *Earth and Planetary Science Letters* 277:443–452.

Qiang, X.-k., Z.-x. Li, C. Powell, and H.-b. Zheng. 2001. Magnetostratigraphic record of the Late Miocene onset of the East Asian monsoon, and Pliocene uplift of northern Tibet. *Earth and Planetary Science Letters* 187:83–93.

Qiu, Z.-x., W.-i. Huang, and Z.-h. Guo. 1987. The Chinese hipparionine fossils. *Palaeontologia Sinica* 175(NS25):1–250.

Qiu, Z.-x. and Z.-d. Qiu. 1990. Neogene local mammalian faunas: Succession and ages. *Journal of Stratigraphy* 14(4):241–260.

Qiu, Z.-x. and Z.-d. Qiu. 1995. Chronological sequence and subdivision of Chinese Neogene mammalian faunas. *Palaeogeography, Palaeoclimatology, Palaeoecolology* 116:41–70.

Qiu, Z.-d., X. Wang, and Q. Li. 2006. Faunal succession and biochronology of the Miocene through Pliocene in Nei Mongol (Inner Mongolia). *Vertebrata PalAsiatica* 44 (2):164–181.

Qiu, Z.-x., W.-y. Wu, and Z.-d. Qiu. 1999. Miocene mammal faunal sequence of China: Palaeozoogeography and Eurasian relationships. In *Land Mammals of Europe*, ed. G. E. Rössner and K. Heissig, pp. 443–457. Munich: Dr. Friedrich Pfeil.

Rea, D. K., H. Snoeckx, and L. H. Joseph. 1998. Late Cenozoic eolian deposition in the North Pacific: Asian drying, Tibetan uplift, and cooling of the northern hermisphere. *Paleoceanography* 13:215–224.

Solounias, N. 1981. The Turolian Fauna from the Island of Samos, Greece. *Contributions to Vertebrate Evolution* 6:1–232.

Steininger, F. F., W. A. Berggren, D. V. Kent, R. L. Bernor, S. Sen, and J. Agustí. 1996. Circum-Mediterranean Neogene (Miocene-Pliocene) marine continental chronologic correlations of European mammal units. In *The Evolution of Western Eurasian Neogene Mammal Faunas*, ed. R. L. Bernor, V. Fahlbusch, and H. W. Mittmann, pp. 7–46. New York: Columbia University Press.

Sun, D., J. Shaw, Z. An, M. Cheng, and L. Yue. 1998. Magnetostratigraphy and paleoclimatic interpretation of a continuous 7.2. Ma Late Cenozoic eolian sediments from the Chinese Loess Plateau. *Geophysical Research Letters* 25:85–88

Vandenberghe, J., H.-y. Lu, D.-h. Sun, J. van Huissteden, and M. Konert. 2004. The Late Miocene and Pliocene climate in East Asia as recorded by grain size and magnetic susceptibility of the Red Clay deposits (Chinese Loess Plateau). *Palaeogeography, Palaeoclimatology, Palaeoecology* 204: 239–255.

Wang, L., H.-y. Lu, N.-q. Wu, J. Li, Y.-p. Pei, G.-b. Tong, and S.-z. Peng. 2006. Palynological evidence for Late Miocene–Pliocene vegetation evolution recorded in the red clay sequence of the central Chinese Loess Plateau and implication for palaeoenvironmental change. *Palaeogeography, Palaeoclimatology, Palaeoecology* 241:118–128.

Wang, X.-m., Z.-d. Qiu, and N. O. Opdyke. 2003. Litho-, bio-, and magnetostratigraphy and paleoenvironment of Tunggur Formation (Middle Miocene) in central Inner Mongolia, China. *American Museum Novitates* 3411:1–31.

Watabe, M. 1992. Phylogeny of Chinese hipparion (Perissodactylia, Mammalia): Their relationships with the western old world and North American hipparionines. *Paleontologia i Evolució* 24/25:155–174.

Wu, N.-q., Y.-p. Pei, H.-y. Lu, Z.-t. Guo, F.-j. Li, and T.-s. Liu. 2006. Marked ecological shifts during 6.2–2.4 Ma revealed by a terrestrial molluscan record from the Chinese Red Clay Formation and implication for Palaeoclimatic evolution. *Palaeogeography, Palaeoclimatology, Palaeoecology* 233:87–299.

Zachos, J., M. Pagani, L. Sloan, E. Thomas, and K. Billups. 2001. Trends, rhythms, and aberrations in global climate 65Ma to present. *Science* 292:686–693.

Zhang, Z. and L. Liu. 2005. The Late Neogene mammal biochronology in the Loess Plateau, China. *Annales de Paléontologie* 91:257–266.

Zhu, Y.-m., L.-p. Zhou, D.-w. Mo, A. Kaakinen, Z. Zhang, and M. Fortelius. 2008. A new magnetostratigraphic framework for late Neogene Hipparion Red Clay in the Eastern Loess Plateau of China. *Palaeogeography, Palaeoclimatology, Palaeoecology* 268:47–57.

APPENDIX

Complete List of the Localities Used in This Study with Geographical Position (Coordinates), Age Correlation (MN-equivalent), Genus-level Faunal Resemblance Indices (Dice, Jaccard, Simpson, and Raup-Crick GFRI), and Mean Hypsodonty Values

Locality	Age (MNEQ)	Latitude	Longitude	T/Dice	T/Jaccard	T/Simpson	T/Raup-Crick	B/Dice	B/Jaccard	B/Simpson	B/Raup-Crick	Mean Hypsodonty
Ad Dabtiyah	4	26.45	48.59	0	0	0	0.0975	0	0	0	0.0525	1.1
Aérotrain	4	48.05	1.85	0	0	0	0.115	0.054054	0.027778	0.125	0.39	1.5
Akcahisar 1	4	38.05	27.62									1
Armantes 1	4	41	–2	0.17647	0.096774	0.375	0.9375	0	0	0	0.075	1.2222
Artenay	4	48.1	1.9	0.11765	0.0625	0.12	0.3025	0.037037	0.018868	0.04	0.0175	1
Artesilla	4	41.18	–1.5	0.13953	0.075	0.17647	0.6125	0.043478	0.022222	0.058824	0.08	1.1111
Baggersee Freudenegg 2	4	48.33	10.01									1
Baggersee Freudenegg 3	4	48.33	10.01									1
Belchatow C	4	51.25	19.33									1
Bézian	4	44.2	0.9	0.23529	0.13333	0.24	0.8675	0.037037	0.018868	0.04	0.025	1.0714
Buñol	4	39.42	0.79	0.093023	0.04878	0.11765	0.2625	0	0	0	0.01	1.1
Can Canals	4	41.2	0.7	0.095238	0.05	0.125	0.3375	0	0	0	0.01	1.1538
Can Julia	4	41.41	1.83	0.057143	0.029412	0.11111	0.335	0.052632	0.027027	0.11111	0.32	1.125
Can Mas	4	41.2	0.7									1
Córcoles	4	40.48	–2.65	0.23529	0.13333	0.5	0.98	0	0	0	0.115	1
Dera Bugti 6	4	29.03	69.15	0.088889	0.046512	0.10526	0.3175	0.041667	0.021277	0.052632	0.0525	1
Eggingen–Mittelhart 3	4	48.36	9.87	0.044444	0.022727	0.052632	0.0625	0.041667	0.021277	0.052632	0.1025	1.1053
El Canyet	4	41.45	1.99	0.054054	0.027778	0.090909	0.2725	0	0	0	0.055	1
Els Casots	4	41.33	2.16	0.10256	0.054054	0.15385	0.5075	0.047619	0.02439	0.076923	0.1625	1
Erkertshofen 2	4	48.97	11.2	0.15385	0.083333	0.23077	0.8	0	0	0	0.04	1
La Romieu	4	44.2	0.9	0.17778	0.097561	0.21053	0.7675	0.041667	0.021277	0.052632	0.0525	1.0714
Langenau 1	4	48.48	10.09	0.12766	0.068182	0.14286	0.4475	0.04	0.020408	0.047619	0.0375	1.0667
Langenau 2	4	48.5	10.1									1
Les Cases de la Valenciana	4	41.2	0.7	0.058824	0.030303	0.125	0.455	0	0	0	0.085	1.1429
Lisboa V	4	38.44	–9.08									1
Mae Soi	4	19.33	97.83									1
Moli Calopa	4	41.33	2.08	0.10526	0.055556	0.16667	0.5525	0.097561	0.051282	0.16667	0.5	1
Montreal-du-Gers	4	43.95	0.2	0.05	0.025641	0.071429	0.24	0	0	0	0.0425	1.4167
Munébrega 1	4	41.25	–2									1.6667
Munébrega 2	4	41.25	–1.7									1
Munébrega 3	4	41.25	–1.7									1
Munébrega AB	4	41.25	–1.7									1
Oberdorf 3 (O3)	4	47.07	15.15									1
Oberdorf 4 (O4)	4	47.07	15.15									1
Pellecahus	4	43.86	0.53	0.20408	0.11364	0.21739	0.7625	0	0	0	0.0025	1.2857
Petersbuch 2	4	48.97	11.19	0.11765	0.0625	0.25	0.7025	0	0	0	0.1075	1
Quinta da Farinheira	4	38.71	–9.13									2
Quinta das Pedreiras	4	38.71	–9.13									1
Quinta Grande	4	38.93	–8.51									2

Rubielos del Mora	4	40.18	−0.66									1
Sihong-qizhui	4	33.16	118.33									1
Sihong-shuanggou	4	33.25	118.2									1
Sihong-songlinzhuang	4	33.3	118.25	0.28571	0.16667	0.375	0.9925	0.088889	0.046512	0.125	0.28	1
Sihong-xiacaowan	4	33.45	109.1									1
Torralba 2	4	40.3	−2.28									1
Wintershof-West	4	48.9	11.16	0.047619	0.02439	0.0625	0.13	0.044444	0.022727	0.0625	0.1275	1
Aktau Mountain	5	44.4	79	0.11765	0.0625	0.25	0.7975	0.054054	0.027778	0.125	0.385	1.1429
Al-Sarrar	5	26.58	48.58	0.21053	0.11765	0.33333	0.94	0.04878	0.025	0.083333	0.205	1
Antonios (ANT)	5	40.3	23	0.055556	0.028571	0.1	0.3375	0.051282	0.026316	0.1	0.27	1
Arroyo del Olivar	5	40.38	−3.65									1.25
Baigneaux-en Beauce	5	48.1	2.15	0.17391	0.095238	0.2	0.6675	0.040816	0.020833	0.05	0.0525	1.1667
Beaugency-Tavers	5	47.78	1.63									1.3333
Belometchetskaja	5	44.6	42	0.26923	0.15556	0.26923	0.9375	0.036364	0.018519	0.038462	0.0125	1.3158
Candir (Loc. 3)	5	40.24	33.48	0.29091	0.17021	0.30769	0.975	0.068966	0.035714	0.068966	0.075	1.4286
Candir (Loc.1)	5	40.29	33.48									1.5
Chios	5	38.36	26.13	0.055556	0.028571	0.1	0.33	0	0	0	0.0725	1.4286
Contres MN 5	5	47.41	1.43	0.25532	0.14634	0.28571	0.9425	0.04	0.020408	0.047619	0.0425	1.0556
Crastes	5	43.73	0.73									1
Dzhilanchik (Uly-Dzhilanchik)	5	49.4	65	0.16667	0.090909	0.3	0.86	0	0	0	0.08	1.25
Edelbeuren-Maurerkopf	5	48.09	10.03	0.058824	0.030303	0.125	0.405	0.054054	0.027778	0.125	0.3375	1
Edelbeuren-Schlachtberg	5	48.09	10.02									1
Eibiswald	5	46.68	15.24									1.2
Engelswies	5	48.03	9.13	0.15385	0.083333	0.23077	0.75	0	0	0	0.0375	1
Estación Imperial (Madrid)	5	40.4	−3.68	0.17143	0.09375	0.33333	0.855	0.10526	0.055556	0.22222	0.6575	1.75
Esvres - Marine Faluns	5	47.3	0.8	0.38235	0.23636	0.5	1	0.028169	0.014286	0.034483	0.0025	1.1111
Faluns of Touraine & Anjou	5	45.5	4.5	0.11765	0.0625	0.25	0.74	0	0	0	0.0875	1.5
Georgensgmünd	5	49.19	11.01	0.11429	0.060606	0.22222	0.6975	0	0	0	0.095	1.25
Gisseltshausen	5	48.7	11.95									1
Grund	5	48.63	16.06									1
Guanghe-dalanggou	5	35.46	103.46									1
Guanghe-wangshijie	5	35.51	103.5									1.4
Göriach	5	47.55	15.3	0.25532	0.14634	0.28571	0.955	0	0	0	0.0025	1
Hambach 6C	5	50.9	6.45	0.14286	0.076923	0.1875	0.615	0	0	0	0.0075	1
Heggbach	5	48.15	9.89	0.16667	0.090909	0.3	0.865	0.051282	0.026316	0.1	0.255	1.1
Henares 2	5	37.6	−1.91									1
Häder	5	48.21	10.38	0.23529	0.13333	0.5	0.98	0	0	0	0.105	1
Kalkaman lake	5	51.7	76.5	0.33333	0.2	0.6	1	0.051282	0.026316	0.1	0.295	1.1111
Karaagac 1	5	39.02	30.04									1
La Hidroelectrica Madrid	5	40.25	−3.43	0.29268	0.17143	0.4	0.98	0.090909	0.047619	0.13333	0.3425	1.2727
La Retama	5	40.1	−2.7	0.15789	0.085714	0.25	0.8	0	0	0	0.035	1.3333

(*continued*)

Locality	Age (MNEQ)	Latitude	Longitude	T/Dice	T/Jaccard	T/Simpson	T/Raup-Crick	B/Dice	B/Jaccard	B/Simpson	B/Raup-Crick	Mean Hypsodonty
Langhian Sables Fauves	5	43.5	0.5									1.3333
Li Mae Long	5	17.71	98.9									1
Luçane	5	43.7	16.62									1.3333
Münzenberg (Leoben)	5	47.4	15.1									1
Mala Miliva	5	44.13	21.43									1
Manchar 1	5	26	68	0.17391	0.095238	0.2	0.695	0.040816	0.020833	0.05	0.055	1.1
Manchar 2	5	26	68	0.15	0.081081	0.21429	0.7325	0.046512	0.02381	0.071429	0.16	1
Manciet base	5	43.81	0.5									1
Montejo de la Vega	5	41.55	–3.65	0.11765	0.0625	0.25	0.77	0.054054	0.027778	0.125	0.3875	1
Moratines	5	40.5	–3.5	0.11765	0.0625	0.25	0.76	0	0	0	0.09	1.6
O'Donnell	5	40.44	–3.59									1.25
PAR-Penuelas (Madrid)	5	40.4	–2.31									1.6667
Paseo de la Esparanza (Madrid)	5	40.4	–3.68	0.11765	0.0625	0.25	0.75	0	0	0	0.125	1.4286
Paseo de la Esparanza 7 (Madri	5	40.4	–3.68									1.6667
Paseo de las Acacias (Madrid)	5	40.4	–2.31	0.16667	0.090909	0.3	0.875	0.10256	0.054054	0.2	0.5475	1.5
Pontlevoy	5	47.4	1.2	0.26415	0.15217	0.26923	0.9525	0.035714	0.018182	0.037037	0.0225	1.0833
Poudenas-Peyrecrechen	5	44.05	0.21	0.21622	0.12121	0.36364	0.93	0	0	0	0.0425	1.0909
Puente de Toledo	5	40.38	–3.7									1.4286
Puente de Vallecas	5	40.2	–3.5	0.29268	0.17143	0.4	0.985	0.045455	0.023256	0.066667	0.115	1
Réaup	5	44.08	0.2									1
Reisensburg	5	48.46	10.3									1
Rimbez - Lapeyrie base	5	44.03	0.03	0.15789	0.085714	0.25	0.805	0	0	0	0.0575	1
Rothenstein 1	5	51.11	7.68	0.10811	0.057143	0.18182	0.565	0.05	0.025641	0.090909	0.2275	1
San Isidro	5	40.4	–3.73									1.25
Sandelzhausen	5	48.62	11.8	0.26087	0.15	0.3	0.97	0.040816	0.020833	0.05	0.045	1.0714
Sant Mamet	5	41.49	2.04	0.15789	0.085714	0.25	0.8	0	0	0	0.0375	1
Savigné-sur-Lathan	5	47.45	0.31	0.14286	0.076923	0.1875	0.615	0	0	0	0.025	1.0556
Seegraben (Leoben)	5	47.4	15.1									1
Shanwang	5	32.01	116.49	0.18605	0.10256	0.23529	0.8375	0.043478	0.022222	0.058824	0.0725	1
Somosaguas-Sur	5	41.49	–2.04									1
Stallhofen	5	46.66	14.13									1
Tarazona	5	41.2	0.5									2
Thymiana B	5	38.31	26.13	0.057143	0.029412	0.11111	0.395	0	0	0	0.0725	1.5
Villafeliche 3	5	41.2	–1.5									1
Voggersberg	5	48.47	12.06									1
Vordersdorf b.Eibiswald	5	46.71	15.23									1
Zhongxiang-Xiaodian	5	31	112.5									1
Ziemetshausen 1b	5	48.3	10.5									1
Zinda Pir 3	5	30.1	70.1	0.057143	0.029412	0.11111	0.3775	0	0	0	0.085	1

Al Jadidah	6	25.5	49.65	0.058824	0.030303	0.125	0.4625	0	0	0	0.1025	1
Arroyo del Val	6	41.3	−1.5	0.17143	0.09375	0.33333	0.885	0	0	0	0.0675	1
Arroyo del Val VI	6	41.18	1.3									1.3333
Ayibaligi mevkii	6	38.52	26.62									3
Castelnau-d'Arbieu	6	43.88	0.7	0.051282	0.026316	0.076923	0.1775	0.047619	0.02439	0.076923	0.1975	1
Catakbagyaka	6	37.12	28.17	0.32432	0.19355	0.54545	0.9975	0.05	0.025641	0.090909	0.2425	1.2222
Devínská Nová Ves - Fissures	6	48.2	17.01	0.21739	0.12195	0.25	0.9025	0.040816	0.020833	0.05	0.065	1
Devínská Nová Ves - Sandhill	6	48.2	17	0.22642	0.12766	0.23077	0.8575	0.071429	0.037037	0.074074	0.0925	1.0833
Elgg	6	47.5	8.86									1
Gallenbach 2b	6	48.4	11.07									1
Haulies	6	43.56	0.66	0.11429	0.060606	0.22222	0.7375	0	0	0	0.08	1
Hezheng-laogou	6	36.46	103.41	0.5	0.33333	0.71429	1	0.093023	0.04878	0.14286	0.38	1.3636
Inönü I (Sinap 24A)	6	40.53	32.64	0.26667	0.15385	0.31579	0.9725	0	0	0	0.015	1.2857
Jiulongkou	6	37	114	0.21622	0.12121	0.36364	0.9225	0.05	0.025641	0.090909	0.2075	1.2222
Junggar-Botamoyin	6	46	89	0.26316	0.15152	0.41667	0.985	0.14634	0.078947	0.25	0.75	1
Junggar-botamoyindong	6	47	89									1
Junggar-chibaerwoyi	6	47	88									1
Junggar-Ganqikairixi	6	46	89									1
Junggar-Tieersihabahe	6	46.66	88.5	0.16216	0.088235	0.27273	0.835	0.05	0.025641	0.090909	0.2575	1
Kentyubek	6	50	65.66									1
Klein Hadersdorf	6	48.6	16.6									1.1429
La Barranca	6	40.75	−4.01									1.5
La Ciesma	6	41.2	0.5									1
Lantian-koujiacun	6	34.16	109.16									1
Laymont	6	43.41	0.98									1
Liet	6	50.6	2.35									1
Liuhe-lingyanshan	6	32	121									1
Lussan	6	43.63	0.73									1
Marciac	6	43.53	0.16									1
Miélan	6	43.43	0.31									1
Montesquiou-sur-L'Osse	6	43.58	0.33									1
Montpezat	6	43.4	0.96									1
Murero	6	41.16	−1.48									1
Póvoa de Satarém	6	38.85	−9.06									1
Paracuellos 3	6	41.3	−1.5	0.17647	0.096774	0.375	0.9375	0.054054	0.027778	0.125	0.3775	1.2
Paracuellos 5	6	40.5	−3.5	0.21053	0.11765	0.33333	0.93	0	0	0	0.0325	1.1111
Pasalar	6	37.43	30.06	0.29508	0.17308	0.34615	0.9475	0.09375	0.04918	0.10345	0.09	1.381
Prebreza	6	43.19	21.15									1.4
Qaidam-Olongbuluk	6	37	97.33									1.4
Rümikon	6	47.38	8.55									1
Riedern	6	47.71	8.3									1

(*continued*)

Locality	Age (MNEQ)	Latitude	Longitude	T/Dice	T/Jaccard	T/Simpson	T/Raup-Crick	B/Dice	B/Jaccard	B/Simpson	B/Raup-Crick	Mean Hypsodonty
Sansan	6	43.9	−0.5	0.35821	0.21818	0.46154	1	0.057143	0.029412	0.068966	0.0025	1
Simorre	6	44	0.3	0.29268	0.17143	0.4	0.9925	0.045455	0.023256	0.066667	0.155	1
Steinberg	6	48.82	10.62									1
Stätzling	6	48.4	10.96	0.31818	0.18919	0.38889	0.995	0	0	0	0.0175	1.05
Tüney	6	40.08	33.61									1
Tairum Nor	6	43.41	113.11	0.4	0.25	0.77778	1	0.052632	0.027027	0.11111	0.37	1.4
Thannhausen	6	48.3	11.5	0.15	0.081081	0.21429	0.6975	0	0	0	0.0125	1.125
Tongxin	6	36.98	105.9	0.28571	0.16667	0.55556	0.995	0	0	0	0.0925	1.3333
Tongxin-dingjiaergou	6	37	106	0.32432	0.19355	0.54545	1	0	0	0	0.0725	1.2857
Tongxin-gujiazhuang	6	37	106									1
Tongxin-jinzuizigou	6	37	106									1
Tongxin-maerzuizigou	6	37	106									1
Tongxin-shataigou	6	37	106									1
Tongxin-Yehuliquezi	6	37	106									1
Trimmelkam	6	48	12.9									1
Wiesholz	6	47.7	8.81									1
Alan (N.D. de Lorette)	7+8	43.21	0.95									1
Alan (Pompat)	7+8	43.21	0.95									1
Aleksandrodar	7+8	47.9	28.5									2
Anwil	7+8	47.37	7.83	0.22857	0.12903	0.44444	0.9575	0	0	0	0.0775	1
Atzgersdorf (WIEN)	7+8	48.1	16.3									1
Bachas	7+8	43.25	0.93									1
Beni Mellal	7+8	32.5	−6.5									1
Can Almirall	7+8	41.2	0.7									1
Can Feliu	7+8	41.5	2.13	0.17647	0.096774	0.375	0.935	0	0	0	0.1025	1
Can Mata 1	7+8	39.98	−5.8									1
Cassagnabère	7+8	43.23	0.8									1
Castell de Barberà	7+8	41.52	2.14	0.29787	0.175	0.33333	0.9875	0.12	0.06383	0.14286	0.4	1
Cerro del Otero	7+8	40.06	−1.01									1
Chiang Muan	7+8	18.93	100.23	0	0	0	0.135	0.054054	0.027778	0.125	0.3675	1.1111
Coca	7+8	41.21	−4.51									1
Coueilles (Baguent)	7+8	43.35	0.88									1
Dang Valley	7+8	28	82.33	0.057143	0.029412	0.11111	0.3875	0.052632	0.027027	0.11111	0.325	1
Dera Bugti W	7+8	29	69									1
Escanecrabe	7+8	43.28	0.75									1
Escobosa	7+8	41.2	0.7									1
Fangxian	7+8	32.1	110.7									1.8
Felsotárkány 3/2 (Güdör-kert)	7+8	47.97	20.41									1
Gebeciler	7+8	38.77	30.75									1.6667

Hachan	7+8	43.28	0.45									1
Hostalets de Pierola Inferior	7+8	41.2	0.5	0.28	0.16279	0.29167	0.9425	0.11321	0.06	0.125	0.275	1
Junggar-duolebulejin	7+8	47	88	0.29412	0.17241	0.625	0.9975	0.054054	0.027778	0.125	0.34	1.57
Junggur_dingshanyanchi	7+8	46.42	87.48									1
Kaiyuan-Xiaolongtan	7+8	23.58	103.25									1
Kutsaj M	7+8	45.4	42.7									1.6667
La Cisterniga	7+8	41.61	–4.68									1
La Grive St. Alban	7+8	44	0	0.26316	0.15152	0.38462	0.895	0.075949	0.039474	0.10345	0.0125	1.1176
Laichingen	7+8	48.5	9.7									1
Lantian-gaopo-64004	7+8	34	109									1.6667
Lantian-gaopo-64008	7+8	34.1	109.3									1.5
Lanzhou-Quantougou	7+8	36.11	103.66									1.6667
Lintong-lengshuigou	7+8	34.1	109.3	0.35294	0.21429	0.75	1	0.054054	0.027778	0.125	0.3625	1.8
Lussan-Adeilhac	7+8	43.25	0.96									1
Mannersdorf	7+8	48	16.5									1.4286
Masquefa	7+8	41.2	0.7									1
Massenhausen	7+8	48.4	11.8	0.26316	0.15152	0.41667	0.985	0.04878	0.025	0.083333	0.2275	1
Minhe-lierbao	7+8	36.6	102.8									1.5
Minhe-nanhawangou	7+8	36.3	102.9									1.5
Minisu de Sus	7+8	46.28	22.01									1
Nombrevilla-2	7+8	41.11	–1.35									1
Opole 2	7+8	50.66	17.91									1
Péguilhan	7+8	43.31	0.7									1
Poudenas-Cayron	7+8	44.05	0.21	0.22857	0.12903	0.44444	0.9775	0	0	0	0.085	1
Przeworno 2	7+8	50.7	17.2									1
Saint-Gaudens (Les Pujaments)	7+8	46.11	0.28									1
Saint-Gaudens (Valentine)	7+8	43.1	0.71									1
Sant Quirze	7+8	41.52	2.08	0.28571	0.16667	0.30435	0.975	0.038462	0.019608	0.043478	0.0375	1
Saricay	7+8	37.33	27.79									1.1667
Serbian lake	7+8	43.83	21.42									1
Siziwangqi-Damiao	7+8	42	111.58									1
Sofca	7+8	39.64	30.17	0.22727	0.12821	0.27778	0.9075	0.085106	0.044444	0.11111	0.205	1.4
Solera	7+8	37.68	–3.35									1
Sopron	7+8	47.68	16.6									1
St. Gaudens	7+8	43.07	0.44									1
St. Stephan im Lavanttal	7+8	46.8	14.9									1
Steinheim	7+8	48.7	10.05	0.22222	0.125	0.23077	0.82	0.035088	0.017857	0.035714	0.01	1.0667
Türkenschanze (WIEN)	7+8	48.23	16.33									1
Toril 3	7+8	41.13	–1.38									1
Tunggur-Moergen	7+8	43	112	1	1	1	1	0.18182	0.1	0.19231	0.6425	1.3529
Xinan	7+8	34.66	112.18									1.6667

(*continued*)

Locality	Age (MNEQ)	Latitude	Longitude	T/Dice	T/Jaccard	T/Simpson	T/Raup-Crick	B/Dice	B/Jaccard	B/Simpson	B/Raup-Crick	Mean Hypsodonty
Yaylacilar	7+8	38.77	30.64									2
Yeni Eskihisar 1	7+8	37.31	28.07									2
Yeni Eskihisar 2	7+8	37.3	28.06									2
Yenieskihisar	7+8	37.31	28.04									2
Amuwusu	9	42.36	112.74									1
Arapli (Igdebaglar)	9	40.65	27.14									1
Atavaska	9	47	28.8	0	0	0	0.1025	0.10526	0.055556	0.22222	0.66	1.3333
Aveiras de Baixo	9	39.11	−8.86									1
Azambujeira inf.	9	39.26	−8.78									1
Ballestar	9	40.4	0.11	0.14634	0.078947	0.2	0.6675	0.13636	0.073171	0.2	0.5875	1.1667
Bermersheim	9	49.77	8.09									1
Bonnefont	9	43.25	0.35									1
Breitenfeld	9	47.16	15.5									1
Buzhor 1	9	46.56	28.16	0.05	0.025641	0.071429	0.1825	0.23256	0.13158	0.35714	0.9475	1.5714
Buzhor 2	9	44.56	28.16									1.5
Can Llobateres I	9	41.2	0.7	0.23188	0.13115	0.30769	0.755	0.16667	0.090909	0.2069	0.27	1.2381
Can Ponsic	9	41.2	0.7	0.21277	0.11905	0.2381	0.815	0.16	0.086957	0.19048	0.6275	1
Can Ponsic I	9	41.53	2.07	0.29091	0.17021	0.30769	0.9725	0.17241	0.09434	0.17241	0.5275	1.1667
Charmoille	9	47.43	7.21	0.1	0.052632	0.14286	0.4275	0.093023	0.04878	0.14286	0.38	1.2308
Creu Conill 20	9	41.67	2									1.4
Das	9	42.35	1.86									1
Dinotheriensande	9	49	8									1
Dongxiang-wangji	9	35.61	103.61									3
Doué-la-Fontaine	9	47.2	−0.3									1
El Firal	9	42.36	1.45	0.2	0.11111	0.28571	0.885	0.18605	0.10256	0.28571	0.8875	1.2308
Eppelsheim	9	49.72	8.97	0.14286	0.076923	0.15385	0.3625	0.16949	0.092593	0.17241	0.4975	1.1905
Esme Akçaköy	9	38.4	28.96	0.052632	0.027027	0.083333	0.225	0.04878	0.025	0.083333	0.23	1.2222
Esselborn	9	49.7	8.1	0.16667	0.090909	0.3	0.8775	0.051282	0.026316	0.1	0.235	1.0909
Estevar	9	0	0	0.11765	0.0625	0.25	0.755	0.21622	0.12121	0.5	0.9675	1.75
Esvres - Upper Faluns	9	47.3	0.8									1.3333
Gaiselberg	9	48.53	16.71									1.3333
Gau-Weinheim	9	49.84	8.04									1.1667
Grakali	9	41.93	44.3									2
Guonigou	9	35.83	103.75	0	0	0	0.12	0.10811	0.057143	0.25	0.755	2.5714
Hammerschmiede	9	47.9	10.61									1
Himberg	9	48.1	16.5									1
Hinterauerbach	9	48.4	12.01									1
Hostalets de Pierola Superior	9	41.2	0.5	0.2439	0.13889	0.33333	0.9475	0.090909	0.047619	0.13333	0.3425	1.2
Höwenegg	9	47.7	8.7	0.11765	0.0625	0.25	0.7925	0.10811	0.057143	0.25	0.735	1.4

Inzersdorf	9	48.13	16.33									2
Isakovo	9	47.22	28.43									1.4
Kalfa	9	46.54	29.23	0.086957	0.045455	0.1	0.2575	0.16327	0.088889	0.2	0.6025	1.1667
Laaerberg	9	48.16	16.4									1.6667
Lantian-12	9	34	109									2
Lapushna	9	46.9	28.5									1
Los Valles de Fuentidueña	9	41	–4.2	0.17778	0.097561	0.21053	0.74	0.20833	0.11628	0.26316	0.8525	1.2222
Mariathal	9	48.6	16.1									2
Masia de la Roma 2	9	40.5	–1									2
Melchingen	9	48.36	9.15									1.3333
Middle Sinap	9	40.56	32.7	0.14286	0.076923	0.1875	0.59	0.13333	0.071429	0.1875	0.615	1.375
Mistelbach	9	48.6	16.5									1
Molina de Aragon	9	40.85	–1.88									2
Nebelbergweg	9	47.38	7.63									1
Nikolsburg	9	48.8	16.63									1.5
Nombrevilla	9	41.07	–1.21	0.16667	0.090909	0.3	0.885	0	0	0	0.08	1.2
Nombrevilla-9	9	41.11	–1.35									1
Oberföhring	9	48.1	11.38									1
Oberhollabrunn	9	48.55	16.06									1
Oshin-II-5 upper	9	47	92.4	0	0	0	0.11	0.16216	0.088235	0.375	0.8925	2.3333
Priay II	9	46	5.3									1
Qaidam-Tuosu	9	37	97	0.15385	0.083333	0.23077	0.7725	0.19048	0.10526	0.30769	0.845	1.6
Rudabánya	9	48.71	20.63	0.14815	0.08	0.15385	0.4425	0.10526	0.055556	0.10714	0.195	1.2222
Salmendingen	9	48.35	9.1									1.3333
Santiga	9	41.2	0.5	0.15385	0.083333	0.23077	0.755	0.047619	0.02439	0.076923	0.175	1.2
Santiga (Sabadell)	9	41.55	2.1									1.2
Seu d'Urgel	9	42.3	1.6									1
Sevastopol (Sebastopol)	9	44.5	33.6	0.15789	0.085714	0.25	0.8075	0.2439	0.13889	0.41667	0.97	1.4444
Sinap 108	9	40.54	32.7									2.3333
Sinap 114	9	40.55	32.71									2
Sinap 14	9	40.53	32.62									2.5
Sinap 4	9	40.55	32.69									1.5
Sinap 64	9	40.56	32.7									2
Sinap 72	9	40.56	32.7	0.058824	0.030303	0.125	0.48	0.21622	0.12121	0.5	0.98	2
Sinap 88	9	40.56	32.7									3
Sinap 8A	9	40.54	32.7									2
Sinap 8B	9	40.54	32.7									2.5
Sinap 91	9	40.55	32.71									2
Sinap 94	9	40.55	32.69									1.5
Sop Mae Tham	9	16.75	99									1.4
Subsol de Sabadell	9	41.33	2.07	0.15	0.081081	0.21429	0.7	0.13953	0.075	0.21429	0.6525	1.3

(*continued*)

Locality	Age (MNEQ)	Latitude	Longitude	T/Dice	T/Jaccard	T/Simpson	T/Raup-Crick	B/Dice	B/Jaccard	B/Simpson	B/Raup-Crick	Mean Hypsodonty
Trie-sur-Baïse	9	43.33	0.36									1
Varnitsa	9	47.2	28.9	0.11429	0.060606	0.22222	0.6775	0.15789	0.085714	0.33333	0.86	1.5
Wartenberg	9	48.4	11.98	0.17647	0.096774	0.375	0.9275	0	0	0	0.11	1.1111
Westhofen	9	49.55	8.25									1
Wuzhong-ganhegou	9	37.99	106.2									1.6667
Vösendorf	9	48.1	16.31	0.057143	0.029412	0.11111	0.3925	0.10526	0.055556	0.22222	0.655	1.25
Zheltokamenka	9	45.26	33.45									1.3333
Zhongning-ganhegou	9	37.49	105.66									2.3333
Berislav	10	46.83	33.42									1.3333
Biru-Bulong	10	31.56	93.83									2.6667
Botamojnak	10	42.95	77.3	0.10811	0.057143	0.18182	0.6075	0.2	0.11111	0.36364	0.9575	2
Can Purull	10	41.55	1.97	0.17021	0.093023	0.19048	0.63	0.28	0.16279	0.33333	0.97	1.3333
Can Trullàs	10	41.55	1.96									1.5
Croix-Rousse	10	45.78	4.83									1
Eldari I	10	41.3	45.7	0.13953	0.075	0.17647	0.6025	0.30435	0.17949	0.41176	0.99	1.4286
Fugu-Laogaochuan-lamagou	10	39	111	0.097561	0.051282	0.13333	0.385	0.40909	0.25714	0.6	1	1.6
Fugu-Laogaochuan-wangdafuliang	10	39	111									1.6
Grebeniki	10	46.88	29.81	0.085106	0.044444	0.095238	0.2	0.36	0.21951	0.42857	1	1.7333
Grossulovo	10	47.35	30									1.75
Guanghe-houshancun	10	35.4833333333333	103.5	0.04878	0.025	0.066667	0.1525	0.31818	0.18919	0.46667	0.9975	1.7
Guanghe-sigou	10	35.48	103.5	0.055556	0.028571	0.1	0.32	0.35897	0.21875	0.7	1	1.2
Gülpinar	10	39.53	26.11	0	0	0	0.0625	0.097561	0.051282	0.16667	0.4525	1.8571
Götzendorf	10	48	16.58	0.10811	0.057143	0.18182	0.5725	0.1	0.052632	0.18182	0.52	1
Hezheng-Dashengou	10	35.85	103.73	0.10714	0.056604	0.11538	0.145	0.40678	0.25532	0.41379	1	1.6111
Kohfidisch	10	47.16	16.35	0.1	0.052632	0.14286	0.4325	0.27907	0.16216	0.42857	0.995	1
La Cantera	10	40.06	–1.01									1.5
La Roma 2	10	40.66	–1.01	0.054054	0.027778	0.090909	0.2825	0.05	0.025641	0.090909	0.215	1.6
La Tarumba I	10	41.55	1.97	0.1	0.052632	0.14286	0.51	0.18605	0.10256	0.28571	0.8875	1.3
Masía del Barbo	10	40.4	–1.1									1.6
Masía del Barbo 2	10	40.66	0.83									1.6
Masía del Barbo 2B	10	40.66	–1.16									1.6
Montredon	10	44.4	3.36	0.1	0.052632	0.14286	0.3825	0.13953	0.075	0.21429	0.63	1.6
Novoukrainka	10	48.3	31.5									1.6667
Orignac	10	43.11	0.16									1.3333
Pentalophos 1 (PNT)	10	41	23	0.093023	0.04878	0.11765	0.375	0.17391	0.095238	0.23529	0.7	1.6364
Poksheshty	10	47.24	28.68	0.15385	0.083333	0.23077	0.79	0.38095	0.23529	0.61538	1	1.875
Ravin de la Pluie (RPL)	10	41	22.95	0.05	0.025641	0.071429	0.205	0.13953	0.075	0.21429	0.6225	1.6667
Ravin des Zouaves 1	10	41	22.95	0	0	0	0.115	0.054054	0.027778	0.125	0.395	2.4
Respopeny	10	47.45	28.36									1.625

Sant Miquel de Taudell	10	41.55	1.98	0.2	0.11111	0.28571	0.905	0.18605	0.10256	0.28571	0.8475	1.3
Sherullah 9	10	34.3	69.4									2
Sinap 1	10	40.54	32.69									1
Sinap 12	10	40.56	32.7	0.088889	0.046512	0.10526	0.255	0.20833	0.11628	0.26316	0.845	1.8462
Sinap 49	10	40.58	32.93	0.097561	0.051282	0.13333	0.39	0.18182	0.1	0.26667	0.7375	1.5882
Sinap 83	10	40.55	32.69									1
Soblay	10	45.1	5.5	0.11765	0.0625	0.25	0.7175	0.054054	0.027778	0.125	0.44	1.6
Stratzing	10	48.45	15.6									1.6667
Terrassa	10	41.56	2	0.17021	0.093023	0.19048	0.655	0.04	0.020408	0.047619	0.05	1.3333
Udabno I	10	41.31	45.23	0.052632	0.027027	0.083333	0.25	0.2439	0.13889	0.41667	0.985	1.4286
Wissberg	10	49.85	8.02	0.23256	0.13158	0.29412	0.9375	0.043478	0.022222	0.058824	0.0825	1
Xirochori 1 (XIR)	10	41	23	0	0	0	0.095	0.15789	0.085714	0.33333	0.845	1.3333
Altan-Teli	11	47	92.6	0	0	0	0.0675	0.25	0.14286	0.45455	0.9825	2.2308
Baccinello V0	11	42.7	11.1									2
Bala Yaylaköy	11	39.74	33.08	0.055556	0.028571	0.1	0.3675	0.10256	0.054054	0.2	0.57	1.4444
Corakyerler	11	40.6	33.63	0.047619	0.02439	0.0625	0.15	0.13333	0.071429	0.1875	0.5375	1.9167
Crevillente 2	11	38.4	-0.5	0	0	0	0.0425	0.046512	0.02381	0.071429	0.16	1.3
Csakvar	11	47.4	18.5	0.042553	0.021739	0.047619	0.0775	0.12	0.06383	0.14286	0.3875	1.7
Darayaspoon	11	38.66	69.86									1
Dorn Dürkheim 1	11	49.77	8.26	0.098361	0.051724	0.11538	0.06	0.125	0.066667	0.13793	0.155	1.25
Dzhuanaryk	11	42.2	75.6	0.11429	0.060606	0.22222	0.7225	0.26316	0.15152	0.55556	0.9925	1.75
Eminova	11	40.11	31.95									1
Garkin	11	38.41	30.31	0.090909	0.047619	0.11111	0.2775	0.34043	0.20513	0.44444	1	1.5
Injana	11	34.33	44.66	0.04878	0.025	0.066667	0.155	0.22727	0.12821	0.33333	0.95	1.6
Kalimanci 1	11	42.5	23.1	0.054054	0.027778	0.090909	0.245	0.1	0.052632	0.18182	0.5075	1.875
Karacahasan	11	39.86	33.24	0	0	0	0.0275	0.34783	0.21053	0.47059	1	1.8889
Kayadibi	11	37.21	30.8	0.1	0.052632	0.14286	0.4475	0.13953	0.075	0.21429	0.6325	1.4167
Kayadibi 3	11	37.59	32.26									1
Kemiklitepe 1.2	11	38.39	29.14	0.042553	0.021739	0.047619	0.055	0.32	0.19048	0.38095	0.9875	1.9286
Kemiklitepe D	11	37.5	29	0.055556	0.028571	0.1	0.325	0.20513	0.11429	0.4	0.955	2
Kocherinovo 1	11	42	23.08									1.75
Kocherinovo 2	11	42.03	23.08									1.6667
Küçükçekmece	11	40.98	28.76	0	0	0	0.0125	0.2449	0.13953	0.3	0.9325	1.3
Lantian-30	11	34	109									2.6667
Lower Maragheh	11	37.41	46.35	0	0	0	0.0875	0.15789	0.085714	0.33333	0.8525	2
Nikiti 1 (NKT)	11	40	23.5	0.054054	0.027778	0.090909	0.2575	0.1	0.052632	0.18182	0.47	1.6
Nikiti 2 (NIK)	11	40	23.5	0	0	0	0.1075	0.10811	0.057143	0.25	0.7075	1.8571
Novaja Emetovka	11	46.65	30.6	0.046512	0.02381	0.058824	0.125	0.30435	0.17949	0.41176	0.97	1.7273
Peralejos D	11	40.48	−1.03									2
Piera	11	41.2	0.5	0.051282	0.026316	0.076923	0.2275	0.095238	0.05	0.15385	0.4025	1.3333
Puente Minero	11	40.36	−1.08	0.095238	0.05	0.125	0.385	0.13333	0.071429	0.1875	0.5825	1.625

(*continued*)

Locality	Age (MNEQ)	Latitude	Longitude	T/Dice	T/Jaccard	T/Simpson	T/Raup-Crick	B/Dice	B/Jaccard	B/Simpson	B/Raup-Crick	Mean Hypsodonty
Qaidam-shenggou	11	37.08	97.25	0.11111	0.058824	0.2	0.635	0.35897	0.21875	0.7	1	1.6667
Ravin des Zouaves 5	11	41	22.95	0.085106	0.044444	0.095238	0.185	0.28	0.16279	0.33333	0.97	1.625
Sabuncubaglari 1	11	41.68	26.59									1
Samos-Q6	11	37.75	26.97									2.2
Samos-Qx	11	37.75	26.97									2
Strumyani 1	11	42.83	23.08									2.25
Strumyani 2	11	42.83	23.1									1.8571
Taghar	11	34.35	69.41									1.75
Thermopigi	11	41.28	23.36	0.045455	0.023256	0.055556	0.1075	0.34043	0.20513	0.44444	0.9975	1.7273
Vivero de Pinos	11	40.33	−1.08									1.5
Yangjiashan	11	35.86	103.76	0.17778	0.097561	0.21053	0.8	0.5	0.33333	0.63158	1	1.25
Yuanmou-baozidong	11	25.66	101.83	0.20513	0.11429	0.30769	0.895	0.19048	0.10526	0.30769	0.8925	1.5
Yulafli (CY)	11	41.2	27.82	0.052632	0.027027	0.083333	0.2175	0.04878	0.025	0.083333	0.19	1.3
Özluce	12	37.24	28.52									2.5
Akgedik-Bayir	12	37.25	28.25	0	0	0	0.045	0.15	0.081081	0.27273	0.785	2.125
Akkasdagi	12	38.49	33.64	0.076923	0.04	0.076923	0.095	0.43636	0.27907	0.46154	1	2.0625
Aljezar B	12	40.33	−1.08									2
Baccinello V2	12	42.7	11.1									1.5
Baltavar	12	47	17	0.047619	0.02439	0.0625	0.18	0.13333	0.071429	0.1875	0.5275	1.5455
Baynunah	12	24.16	52.56	0.051282	0.026316	0.076923	0.2375	0.2381	0.13514	0.38462	0.9675	1.5
Belka	12	50.81	28.18	0.1	0.052632	0.14286	0.4475	0.27907	0.16216	0.42857	1	1.375
Casa del Acero	12	38.1	−0.5									1.6667
Casteani	12	42.5	11.15									1.4
Cerro de la Garita	12	40.38	−1.08	0.11321	0.06	0.11538	0.2425	0.25	0.14286	0.25926	0.9375	1.2308
Chimishlija (Cimislia)	12	46.5	28.8	0.081633	0.042553	0.086957	0.1575	0.30769	0.18182	0.34783	0.985	1.4737
Chobruchi (Tchobroutchi)	12	46.6	29.7	0.090909	0.047619	0.11111	0.3175	0.25532	0.14634	0.33333	0.925	1.7143
Chomateres	12	38.08	23.88	0.10526	0.055556	0.16667	0.535	0.097561	0.051282	0.16667	0.5	1.4
Çobanpinar (Sinap 42)	12	40.21	32.53	0	0	0	0.0375	0.18605	0.10256	0.28571	0.825	1.8
Concud	12	40.4	−1.13	0.086957	0.045455	0.1	0.21	0.16327	0.088889	0.2	0.615	1.2727
Concud Barranco	12	40.4	−1.01									1.5
Crevillente 15	12	38.25	−0.8									1.375
Crevillente 16	12	38.23	−0.8	0	0	0	0.1	0.054054	0.027778	0.125	0.3625	1.3333
Duzyayla	12	39.92	37.31	0	0	0	0.105	0.15789	0.085714	0.33333	0.87	1.4286
Ebic	12	38.8	35.65									1.5
Elekci	12	37.34	28.17									1.6667
Fiume Santo	12	40.8	8.3									1.6667
Gura-Galben	12	46.42	28.42	0	0	0	0.07	0.21053	0.11765	0.44444	0.9725	1.5556
Hadjidimovo-1	12	41.5	23.83	0.11111	0.058824	0.11538	0.1775	0.2807	0.16327	0.28571	0.9475	1.4762
Halmyropotamos (HAL)	12	38.5	24.2	0.043478	0.022222	0.05	0.065	0.20408	0.11364	0.25	0.805	1.6429

Jilong	12	28.86	85.18									1.8
Kalimanci 2	12	42.5	23.1	0.047619	0.02439	0.0625	0.135	0.13333	0.071429	0.1875	0.57	1.7
Kalimanci 4	12	42.5	23.1									2.25
Kalimantsi-Pehtsata	12	42.5	23.1									1.3333
Kavakdere (Turolian)	12	40.24	32.56									1.75
Kemiklitepe A-B	12	37.5	29	0.04878	0.025	0.066667	0.1675	0.18182	0.1	0.26667	0.8175	2
Kerassia 1	12	38.5	23	0.10526	0.055556	0.16667	0.4925	0.2439	0.13889	0.41667	0.97	1.6667
Kerassia 4	12	38.5	23	0.057143	0.029412	0.11111	0.365	0.26316	0.15152	0.55556	0.9925	1.25
Kizilören	12	37.85	32.1	0	0	0	0.075	0.15789	0.085714	0.33333	0.9	1.3333
Kromidovo 2	12	41.45	23.36									2
Lantian-6	12	34	109	0.11111	0.058824	0.2	0.6375	0.25641	0.14706	0.5	0.99	2.3333
Las Pedrizas	12	36.83	−4.5									1.6667
Los Aljezares	12	37.75	-0.85	0.058824	0.030303	0.125	0.395	0.10811	0.057143	0.25	0.7225	1.5
Los Mansuetos	12	40.35	−1.11	0.12	0.06383	0.125	0.315	0.33962	0.20455	0.375	0.99	1.4545
Lufeng-shihuiba	12	25.3	102.4	0.13793	0.074074	0.15385	0.2725	0.22951	0.12963	0.24138	0.765	1
Mahmutgazi	12	38.02	29.4	0.054054	0.027778	0.090909	0.3075	0.2	0.11111	0.36364	0.9425	1.6667
Masada del Valle 2	12	40.38	−0.43									2
Middle Maragheh	12	37.4	46.36	0.071429	0.037037	0.076923	0.0575	0.27119	0.15686	0.27586	0.915	2
Molayan	12	34.31	69.41	0.047619	0.02439	0.0625	0.13	0.31111	0.18421	0.4375	0.995	1.25
Montemassi	12	42.9	11									2
Mt. Luberon	12	43.7	5.4	0	0	0	0.1275	0.21622	0.12121	0.5	0.9575	1.75
Mytilinii 1A	12	37.75	26.96	0.05	0.025641	0.071429	0.2025	0.23256	0.13158	0.35714	0.9325	2.1111
Mytilinii 1B	12	37.75	26.96	0.054054	0.027778	0.090909	0.2825	0.2	0.11111	0.36364	0.9275	2
Mytilinii 1C	12	37.75	26.96									1
Mytilinii 3	12	37.75	26.96									2.5
Mytilinii 4	12	37.75	26.96									2
Novo-Elizavetovka	12	47	31	0.093023	0.04878	0.11765	0.3425	0.30435	0.17949	0.41176	0.9975	1.5
Ortok	12	42.4	75.6	0.057143	0.029412	0.11111	0.3675	0.26316	0.15152	0.55556	1	1.7143
Perivolaki	12	38.41	23.5	0.040816	0.020833	0.043478	0.045	0.26923	0.15556	0.30435	0.955	1.8333
Pikermi	12	38.01	23.99	0.11111	0.058824	0.15385	0.08	0.34667	0.20968	0.44828	0.99	1.48
Pikermi-MNHN (PIK)	12	38.08	23.88									1.5
Pinaryaka	12	41.19	32.49	0	0	0	0.065	0.20513	0.11429	0.4	0.95	1.2
Prochoma	12	41	22.93	0.04878	0.025	0.066667	0.1475	0.18182	0.1	0.26667	0.8075	1.5455
Ravin X	12	38.4	23.48	0	0	0	0.04	0.18605	0.10256	0.28571	0.8575	1.5
Ribolla	12	43	11.1									2
Salihpasalar	12	37.25	28.27	0.052632	0.027027	0.083333	0.2375	0.2439	0.13889	0.41667	0.98	1.6667
Salihpasalar 1	12	37.25	28.25	0.055556	0.028571	0.1	0.3175	0.35897	0.21875	0.7	1	1.5714
Salihpasalar 2	12	37.25	28.26	0.055556	0.028571	0.1	0.2975	0.35897	0.21875	0.7	1	1.5
Samos	12	37.75	26.97	0.081633	0.042553	0.086957	0.175	0.15385	0.083333	0.17391	0.4725	1.7407
Samos (A-1)	12	37.75	26.97	0.072727	0.037736	0.076923	0.0975	0.34483	0.20833	0.34483	0.99	1.9231
Samos Main Bone Beds	12	37.5	26.87	0.055556	0.028571	0.076923	0.005	0.34667	0.20968	0.44828	0.9875	1.9697

(*continued*)

Locality	Age (MNEQ)	Latitude	Longitude	T/Dice	T/Jaccard	T/Simpson	T/Raup-Crick	B/Dice	B/Jaccard	B/Simpson	B/Raup-Crick	Mean Hypsodonty
Samos Old Mill Beds	12	37.5	26.87									2.5
Samos White Sands	12	37.5	26.87									2.2
Samos-Q5	12	37.75	26.97									1.875
Sandikli Kinik	12	38.56	30.13	0.097561	0.051282	0.13333	0.37	0.45455	0.29412	0.66667	1	2
Serefköy	12	37.36	28.23	0.052632	0.027027	0.083333	0.2525	0.19512	0.10811	0.33333	0.905	1.8
Serrazzano	12	43.6	10.8									2
Sinap 26	12	40.56	32.64	0.10811	0.057143	0.18182	0.565	0.2	0.11111	0.36364	0.91	1.9
Sinap 27	12	40.56	32.64									2.25
Sinap 33	12	40.55	32.64	0.055556	0.028571	0.1	0.3075	0.20513	0.11429	0.4	0.945	1.8
Sinap 70	12	40.55	32.64									2.5
Sor	12	39.27	67.65	0.054054	0.027778	0.090909	0.285	0.3	0.17647	0.54545	0.995	1.7143
Taraklia	12	46.5	29	0.075472	0.039216	0.076923	0.12	0.39286	0.24444	0.40741	1	1.7917
Tudorovo	12	46.26	30.03	0	0	0	0.105	0.27027	0.15625	0.625	0.9975	1.6667
Upper Maragheh	12	37.4	46.41	0.088889	0.046512	0.10526	0.2675	0.33333	0.2	0.42105	1	1.9091
Valdecebro 5	12	40.35	–1.03									2
Vathylakkos 1 (VLO)	12	41	23									1.6667
Vathylakkos 2 (VTK)	12	41	23	0	0	0	0.07	0.097561	0.051282	0.16667	0.5075	1.5556
Vathylakkos 3 (VAT)	12	41	23	0	0	0	0.02	0.2	0.11111	0.2381	0.76	1.4667
Almenara-Casablanca M	13	40	0									1
Amasya 2	13	37.65	28.48									2
Ananjev	13	47.7	30									1.5
Arenas del Rey	13	36.96	–3.9									2
Arquillo 1	13	40.4	–1.1	0.090909	0.047619	0.11111	0.285	0.29787	0.175	0.38889	0.9875	2
Baccinello V3	13	42.7	11.1	0.051282	0.026316	0.076923	0.21	0.28571	0.16667	0.46154	0.9875	1.6
Brisighella	13	44.5	11.6	0	0	0	0.0575	0.2439	0.13889	0.41667	0.985	1.9091
Bunker de Valdecebro	13	40.35	–1.05									3
Douaria	13	35	10									1.5
Dytiko 1 (DTK)	13	41	23	0	0	0	0.0275	0.13636	0.073171	0.2	0.63	1.8462
Dytiko 2 (DIT)	13	41	23	0.055556	0.028571	0.1	0.3225	0.15385	0.083333	0.3	0.8575	1.5
Dytiko 3 (DKO)	13	41	23	0	0	0	0.045	0.05	0.025641	0.090909	0.2	1.6667
El Arquillo 1	13	40.35	–1.05	0.086957	0.045455	0.1	0.21	0.28571	0.16667	0.35	0.9675	1.9333
Fugu-Laogaochuan-miaoliang	13	39	111	0.057143	0.029412	0.11111	0.3725	0.36842	0.22581	0.77778	1	1.3333
Gravitelli	13	38.2	15.5	0.11111	0.058824	0.2	0.65	0.30769	0.18182	0.6	0.9975	1.6667
Gusinyy perelyot	13	50.25	67.83	0.085106	0.044444	0.095238	0.2025	0.44	0.28205	0.52381	1	2.1
Hatvan	13	47.66	19.68									1.25
Hsin-An-Loc.12	13	34.6	112.2	0.10526	0.055556	0.16667	0.5375	0.4878	0.32258	0.83333	1	1.2857
Kalmakpaj	13	47.3	85.3	0.095238	0.05	0.125	0.385	0.44444	0.28571	0.625	1	2.2
Karabastuz	13	50.3	79.16	0.057143	0.029412	0.11111	0.3525	0.26316	0.15152	0.55556	0.9925	2
Khirgis-Nur II-lower	13	49.2	93.4	0	0	0	0.1225	0.27027	0.15625	0.625	0.995	2.3333

Kholobolochi Nor	13	45.4	100.9									2
Krivaja Balka	13	46.5	30.8									1
La Alberca	13	38	–0.6									2
La Gloria 5	13	40.38	–1.06									3
Lantian-42	13	34	109	0.10811	0.057143	0.18182	0.615	0.55	0.37931	1	1	1.571
Lantian-44	13	34	109									1
Las Casiones	13	40.43	–1.11	0.044444	0.022727	0.052632	0.0575	0.16667	0.090909	0.21053	0.7275	2
Librilla	13	38	-0.6									2.2
Milagros	13	41.35	–3.41	0	0	0	0.08	0.21053	0.11765	0.44444	0.9775	2
Nurpur	13	32	77	0.088889	0.046512	0.10526	0.265	0.125	0.066667	0.15789	0.45	1.4
Odessa 2	13	46.5	30.8									2.5
Olkhon (Sarayskaya. hor. 3)	13	53.1	107.2									1
Pao-Te-Lok.108	13	39	111	0.097561	0.051282	0.13333	0.3925	0.54545	0.375	0.8	1	1.75
Pao-Te-Lok.109	13	39	111	0.054054	0.027778	0.090909	0.2875	0.55	0.37931	1	1	1.5
Pao-Te-Lok.110	13	39	111	0.055556	0.028571	0.1	0.32	0.35897	0.21875	0.7	1	1.8
Pao-Te-Lok.30	13	39	111	0.081633	0.042553	0.086957	0.2025	0.53846	0.36842	0.6087	1	2
Pao-Te-Lok.31	13	39	111	0.095238	0.05	0.125	0.3575	0.35556	0.21622	0.5	0.9975	1.875
Pao-Te-Lok.43	13	39	111	0.045455	0.023256	0.055556	0.0975	0.51064	0.34286	0.66667	1	1.75
Pao-Te-Lok.44	13	39	111	0.1	0.052632	0.14286	0.4675	0.51163	0.34375	0.78571	1	1.7647
Pao-Te-Lok.49	13	39	111	0.18182	0.1	0.19231	0.6425	1	1	1	1	1.4375
Pao-Te-Lok.52	13	39	111	0	0	0	0.0975	0.36842	0.22581	0.77778	1	1.5
Pavlodar	13	52	77	0.081633	0.042553	0.086957	0.175	0.42308	0.26829	0.47826	1	2
Polgardi	13	47	18.3	0	0	0	0.0225	0.13636	0.073171	0.2	0.63	1.5
Qingyang-Lok.115	13	36	108	0.10526	0.055556	0.16667	0.505	0.53659	0.36667	0.91667	1	1.875
Qingyang-Lok.116	13	36	108	0.10256	0.054054	0.15385	0.4825	0.47619	0.3125	0.76923	1	1.8889
Rambla de Valdecebro 0	13	40.22	–1.05									3
Rambla de Valdecebro 3	13	40.22	–1.05									2.6667
Rambla de Valdecebro 6	13	40.22	–1.05									2.3333
Sahabi	13	30.08	20.75									1.5
Saint Arnaud	13	36.08	5.4									2.3333
Songshan-Loc.2	13	36.96	103.29	0.18605	0.10256	0.23529	0.8275	0.3913	0.24324	0.52941	1	1.4444
Songshan-Loc.3	13	36.96	103.27	0.15789	0.085714	0.25	0.805	0.43902	0.28125	0.75	1	1.4286
Taskinpasa 1	13	38.49	34.94									2
Tha Chang 2	13	15	102.33	0	0	0	0.08	0.052632	0.027027	0.11111	0.315	2
Valdecebro 3	13	40.35	–1.08									2.25
Venta del Moro	13	39.4	–0.4	0	0	0	0.01	0.23529	0.13333	0.27273	0.8825	1.8182
Villastar	13	40.01	–1.01									2.4
Wu-Hsiang-Loc.71	13	36.8	112.8									1
Wu-Hsiang-loc.78	13	36.8	112.9									1.4286
Wu-Hsiang-Lok.70	13	36.8	112.9									1.4286
Wu-Hsiang-Lok.73	13	39	111	0	0	0	0.1	0.42105	0.26667	0.88889	1	1.25

(*continued*)

Locality	Age (MNEQ)	Latitude	Longitude	T/Dice	T/Jaccard	T/Simpson	T/Raup-Crick	B/Dice	B/Jaccard	B/Simpson	B/Raup-Crick	Mean Hypsodonty
Yushe-hounao	13	37	112.9	0	0	0	0.0525	0.2439	0.13889	0.41667	0.99	1.5
Alcoy	14	38.6	–0.5	0	0	0	0.09	0.15385	0.083333	0.3	0.8275	2
Celleneuve	14	43.5	3.5									1.6667
Chono Hariah 1 lower	14	48.3	93									3
Dorkovo	14	42.03	24.13	0	0	0	0.12	0.10811	0.057143	0.25	0.695	1.5
Fonelas	14	37.25	–3.1	0	0	0	0.025	0.095238	0.05	0.15385	0.405	2
Gödöllö	14	47.6	19.36									1.5
Gaozhuang	14	38.28	113.11	0	0	0	0.065	0.04878	0.025	0.083333	0.2675	2
Gorafe 1	14	37.29	–3.02									1
Gorafe 4	14	37.29	–3.02									2
Guanghe-shilidun-LX200014	14	35.5	103.5	0.054054	0.027778	0.090909	0.285	0.3	0.17647	0.54545	0.995	1.86
Kessani 1.2	14	41	25									1
Khirgis-Nur II	14	49.2	93.4	0.055556	0.028571	0.1	0.2725	0.051282	0.026316	0.1	0.3075	2.5
Khirgis-Nur II-upper	14	49.2	93.4	0	0	0	0.0825	0.26316	0.15152	0.55556	1	2.4
Kosyakino	14	43.9	46.68	0	0	0	0.04	0.23256	0.13158	0.35714	0.9525	1.2857
La Gloria	14	40.23	–5.48									1.6667
La Gloria 4	14	40.38	–1.06	0	0	0	0.0925	0.15385	0.083333	0.3	0.81	2
Montpellier	14	43.6	3.89	0	0	0	0.0125	0.24	0.13636	0.28571	0.8875	1.4615
Olkhon (Sarayskaya. hor. 5)	14	53.1	107.2									2
Orrios	14	40.35	–1									2
Peralejos	14	40.29	–1.02									1
Peralejos E	14	40.48	–1.03									1
Saint Laurent des Arbres	14	43.93	4.8									1.6667
Trévoux	14	45.93	4.76									1.4

Vendargues	14	43.65	3.96									2
Villeneuve de la Raho	14	42.63	2.91									1.5
Yushe-Gaozhuang	14	37	113	0	0	0	0.0525	0.047619	0.02439	0.076923	0.1675	2
Anvers 1	15	51.21	4.41									1
Apolakkia	15	36.06	27.8									1.6667
Çalta 2	15	40.23	32.54	0	0	0	0.0225	0.13953	0.075	0.21429	0.69	2
Capeni	15	46.01	25.55	0	0	0	0.03	0.13953	0.075	0.21429	0.625	1
Ciuperceni 2	15	44.19	25.22									1
Csarnota 2	15	45.89	18.21	0	0	0	0.045	0.04878	0.025	0.083333	0.1925	1
Ivanovce	15	48.2	17.9	0	0	0	0.0475	0.1	0.052632	0.18182	0.485	1.2
La Calera	15	39.31	–5.15	0	0	0	0.0525	0.15	0.081081	0.27273	0.7375	1.2
Layna	15	41.05	–2.19	0	0	0	0.0825	0.15	0.081081	0.27273	0.775	2.1667
Malushteni	15	46.13	28.08	0	0	0	0.0675	0.097561	0.051282	0.16667	0.4225	1.6667
Megalo Emvolon (MEV)	15	40.3	22.45									2
Mianxian-yangjiawan	15	33.16	106.7	0	0	0	0.0775	0.15385	0.083333	0.3	0.81	1.4
Muselievo	15	43.3	24.4	0	0	0	0.0825	0.15385	0.083333	0.3	0.8475	1.1667
Odessa Catacombs	15	46.5	30.8	0	0	0	0.035	0.13333	0.071429	0.1875	0.53	1.6667
Perpignan	15	42.68	2.88	0	0	0	0.01	0.15385	0.083333	0.17391	0.48	1.5
Sugas-Bai	15	45.5	25.5									1
Val di Pugna	15	43.3	11.5									1.6667
Varghis	15	46.13	25.53									1
Weze 1	15	50.08	18.78	0.054054	0.027778	0.090909	0.2825	0.15	0.081081	0.27273	0.81	1
Wölfersheim	15	50.4	8.85	0	0	0	0.07	0.05	0.025641	0.090909	0.245	1.25

NOTE: T = similarity with Tunggur-Moergen; B = similarity with Baode locality 49. Localities with blank GFRI values had fewer than seven distinctive genera and were not used in similarity analysis.

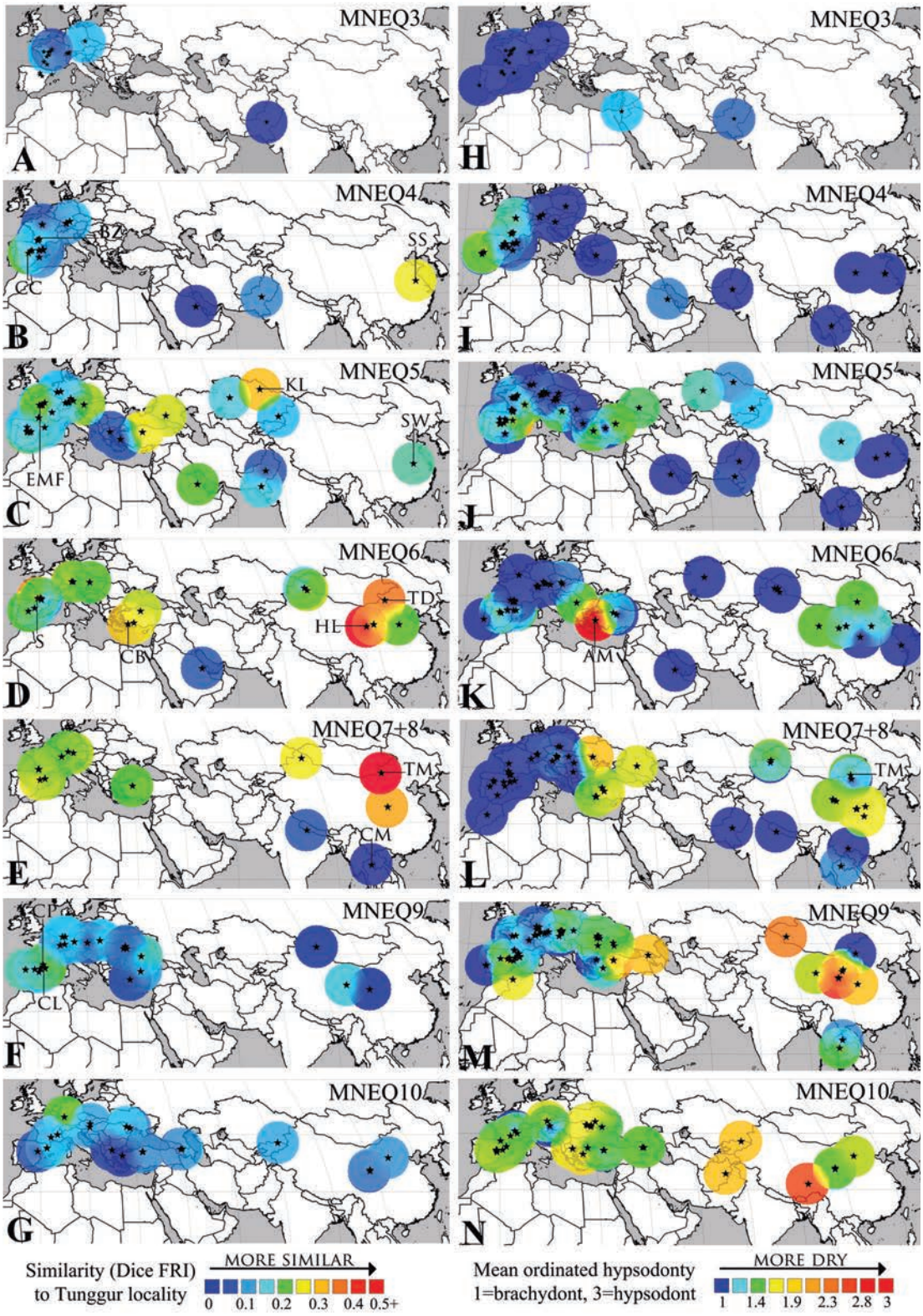

Plate 29.1 Dice similarity index values at the genus level (Dice FRI) of the Eurasian localities compared to Tunggur-Moergen (*A*–*G*) and their mean ordinated hypsodonty (Hypso) values (*H*–*N*) mapped as a grid for MNEQ 3 to MNEQ 10 time intervals. (*A*) Dice FRI-MNEQ 3; (*B*) Dice FRI-MNEQ 4; (*C*) Dice FRI-MNEQ 5; (*D*) Dice FRI-MNEQ 6; (*E*) Dice FRI-MNEQ 7+8; (*F*) Dice FRI-MNEQ 9; (*G*) Dice FRI-MNEQ 10. Yellow/red patterns in *A*–*G* indicates high similarity to Tunggur locality, while blue represents low similarity; (*H*) Hypso-MNEQ 3; (*I*) Hypso-MNEQ 4; (*J*) Hypso-MNEQ 5; (*K*) Hypso-MNEQ 6; (*L*) Hypso-MNEQ 7+8; (*M*) Hypso-MNEQ 9; (*N*) Hypso-MNEQ 10. Yellow/red pattern in *H*–*N* indicates increased aridity, while blue represents high humidity. SS = Sihong-Songlinzhuang, China; CC = Córcoles, Spain; BZ = Bézian, France; EMF = Esvres–Marine Faluns, France; KL = Kalkaman Lake, Kazakhstan; SW = Shanwang, China; TD = Tongxin-Dingjiaergou, China; HL = Hezheng-Laogou, China; S = Sansan, France; CB = Catakbagyaka, Turkey; AM = Ayibaligi Mevkii, Turkey; TM: Tunggur-Moergen, China; CM = Chiang Muan, Thailand; CP = Can Ponsic I, Spain; CL = Can Llobateres I, Spain.

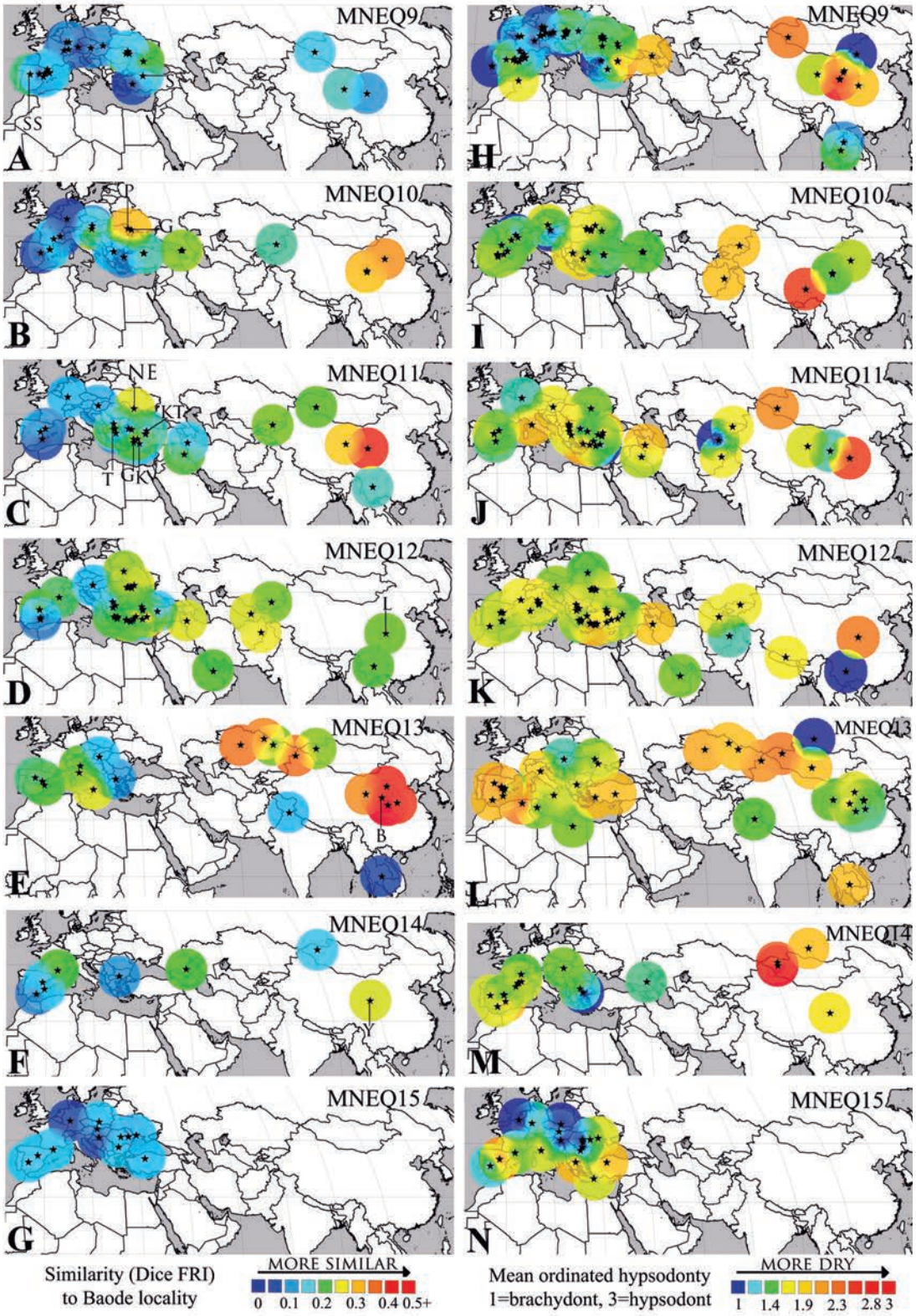

Plate 29.2 Dice similarity index values at the genus level (Dice FRI) of the Eurasian localities compared to Baode locality 49 (*A*–*G*) and their mean ordinated hypsodonty (Hypso) values (*H*–*N*) mapped as a grid for MNEQ 9 to MNEQ 15 time intervals. (*A*) Dice FRI-MNEQ 9; (*B*) Dice FRI-MNEQ 10; (*C*) Dice FRI-MNEQ 11; (*D*) Dice FRI-MNEQ 12; (*E*) Dice FRI-MNEQ 13; (*F*) Dice FRI-MNEQ 14; (*G*) Dice FRI-MNEQ 15. Yellow/red pattern in *A*–*G* indicates high similarity to Baode loc. 49, while blue represents low similarity. (*H*) Hypso-MNEQ 9; (*I*) Hypso-MNEQ 10; (*J*) Hypso-MNEQ 11; (*K*) Hypso-MNEQ 12; (*L*) Hypso-MNEQ 13; (*M*) Hypso-MNEQ 14; (*N*) Hypso-MNEQ 15. Yellow/red pattern in *H*–*N* indicates increased aridity, while blue represents high humidity. S = Sinap, Turkey; SS = Subsol de Sabadell, Spain; G = Grebeniki, Ukraine; P = Poksheshty, Moldova; K = Karacahasan, Turkey; KT = Kemiklitepe 1–2, Turkey; G = Garkin, Turkey; T = Thermopigi, Greece; NE = Novaja Emetovka, Ukraine; L = Lantian, China; B = Baode locality 49, China; Y = Yushe, China.